Advances in soil reinforcement with geosynthetics: from laboratory tests to design practice

Giuseppe Cardile,* Marilene Pisano**

Summary

This paper provides an updated overview on the role of geosynthetics with reinforcement function in order to define sustainable development strategies. Considering the extent of the subject, the field will be restricted to some applications, such as geosynthetic-reinforced soil (GRS) walls and steep slopes, where the structure is built by alternating layers of compacted soil and polymeric reinforcements wrapped around the face of the structure or connected to the facing (cast-in-place concrete facing or facing assembled with precast concrete blocks or panels).

Whether it is intended as execution of laboratory tests on the representative elementary volume or as analysis of the behaviour of instrumented full-scale geosynthetic reinforced soil structures, for this discipline experimentation represented, and it still does, the starting point and the driving force behind the continuous progresses. For these reasons, this paper will be developed starting from results that recent research has produced on the definition of short- and long-term design parameters, both studied in laboratory through large-scale (frequently prototype) test apparatus. The obtained results will be explained by taking into account the interaction mechanisms actually mobilised along the soil-geosynthetic interface. Thereafter, the authors will analyse how these research advances have resulted or could result in advancement in the design practice.

Keywords: geosynthetics, geogrid, pullout, cyclic loading, soil-reinforcement interface, design parameters, apparent coefficient of friction, viscous properties, geosynthetic-reinforced soil walls, reinforced steep slopes.

1. Introduction

More than forty years ago, the great impulse given by producers of polymeric materials has allowed developing new building materials, functionalizing them to many civil and environmental engineering applications, and this has been possible even through the synergy between academic world, manufacturers and stakeholders.

The connection between geosynthetics engineering and geotechnical engineering has become inescapable. Nowadays in fact, geosynthetics pervade most branches of the geotechnical engineering and a continuous growth of knowledge has developed over years, enabling to translate research into innovation.

In this context, the authors will try to analyse some questions still open, whose answers could have important consequences especially on two aspects: the first aspect is related to a more conscious territory development and protection, achieved in full respect of social and environmental sustainability; the second one concerns the drafting and upgrade of technical recommendations that can reassure and guide the designer towards the choice of these solutions. The paper is based on the Keynote Lecture delivered for the 7th edition of the Italian National Congress of Geotechnical Researchers (CNRIG2019) entitled "The Geotechnical Research for the Protection and Development of the Territory" (Lecco Campus, July 3rd to 5th 2019).

2. Geosynthetics as solutions for sustainability challenges

From a design point of view, engineering applications with geosynthetics represent a sustainable and mature technological solution nowadays.

Worldwide, we are witnessing the demonization of plastics used to make "single-use plastics" and the consequent microplastics responsible of a pollution process, which causes serious risks for environment. Geosynthetics, which are building materials used in engineering applications characterised by a long service life, represent the winning solution in

* Associate Professor of Geotechnical Engineering, Ph.D., Mediterranea University of Reggio Calabria, Department of Civil Engineering, Energy, Environment and Materials (DICEAM), Italy

** Research assistant in Geotechnical Engineering, Ph.D., Mediterranea University of Reggio Calabria, Department of Civil Engineering, Energy, Environment and Materials (DICEAM), Italy

terms of sustainable development that is a *development that meets the needs of the present without compromising the ability of future generations to meet their own needs* (World Commission on Environment and Development, 1987).

With reference to the Unite Nations Program *2030 Agenda*, developed to transform our world in a sustainable way and aimed at ending poverty in all its forms, geosynthetics can represent a solution to reach the established goals (*i.e.* clean water and sanitation; industry, innovation and infrastructure; responsible consumption and production; climate action; partnership for the goal).

Climate change is the principal cause for increasing natural disasters (typhoons, landslides, flood, etc.) which are becoming more frequent and stronger. It can have a significant impact on human health, food production and nutrition, migration, economic and political global equilibrium. In the coming years, reducing greenhouse gas emissions (GHGs), mainly carbon dioxide (CO_2), will be necessary and urgent. To analyse properly the environmental impact of a system or a product generally related to the generated CO_2 emissions, it is necessary to carry out this evaluation by referring to its overall life cycle (Life Cycle Assessment, LCA). Therefore, the process starting from the extraction of the raw material must be considered; such material passes through the industrial production until it can be used as a specific application afterwards; finally, a possible recycling and its waste final disposal have to be taken into account. In these analyses, indicators that refer to numerous factors (such as the complex energy supply and demand, climate change, ozone formation, particulate formation, acidification, eutrophication, land use, water resource, human health, biodiversity protection and resources availability) must be used. In recent years, several LCA analyses carried out on different geosynthetics' applications have shown that geosynthetics represent technological solutions capable to reduce the emissions of produced GHGs dramatically, compared to the traditional geotechnical structures [WALLBAUM *et al.*, 2014].

Moreover, geosynthetics can intervene on adaptation to climate change in progress. Adaptation means anticipating the adverse effects of climate change and taking appropriate actions to prevent or minimise the damage they can cause. It has been shown that a well-planned, early adaptation action saves money and lives afterwards. Geosynthetics use (*i.e.* passive structural barriers for landslide risk mitigation; embankments for flood protection, for the construction of dams and levees; solutions for erosion risk prevention; earth structures for re-profiling a slope; etc.) gives an important contribution in increasing the community resilience of infrastructural and geotechnical structures against, for instance, earthquakes, floods, landslides and drought.

The construction methods of geosynthetic-reinforced soil structures allow a substantial decrease in execution time by virtue of their ease of execution in comparison to traditional techniques (lower costs for skilled workers as well as for the hire of vehicles and equipment). Specifically, the economic saving obtained in the short-term by using geo-reinforcements in a retaining wall, compared to the more conventional reinforced concrete technologies, varies between 25% and 50%. Frequently, it is possible to reduce construction cost substantially by using the granular soil available on site or a part of it (this entailing the advantage of cancelling or reducing site-quarry transport costs). Moreover, geosynthetics in road and railway embankments allow a steeper batter and consequently savings for expropriation fees.

Geosynthetics solutions ensure considerable cost saving even during the service life (in the long-term period), measurable both in the lower maintenance required and in the best performances offered, especially during seismic events. After seismic events of high magnitude, geosynthetic-reinforced soil (GRS) walls showed a better behaviour compared to traditional walls: these evidences have been confirmed and well documented [WHITE and HOLTZ, 1994; TATSUOKA *et al.*, 1995, 1997; SANDRI, 1997; HUANG, 2000; KOSEKI *et al.*, 2000; LING *et al.*, 2001; FANG *et al.*, 2003; HUANG and WANG, 2005; LING and LESHCHINSKY, 2005; KOSEKI *et al.*, 2006; WARTMAN *et al.*, 2006; KUWANO *et al.*, 2014] on the occasion of different seismic events. During the seismic event that hit the Japanese Pacific coast (Tōhoku Earthquake, 2011), which represents one of the most violent earthquakes ever recorded in urbanized areas (having a magnitude of $M_w = 9.0$), only 1% of the approximately 1600 reinforced earth structures being analysed post-earthquake proved to be seriously damaged, while about 90% of them showed no damage [KUWANO *et al.*, 2014]. This better behaviour is due to the high dissipation of energy produced by the sequential activation of internal plastic mechanisms and to an overall more ductile behaviour deriving from large deformations allowed by the structure itself [MASINI *et al.*, 2015]. In reinforced retaining walls or reinforced steep slopes, the phenomena of complete collapse in seismic conditions have been rare, unless phenomena of dynamic liquefaction of the foundation soils or excessive development of settlements caused by the seismic motion occur at the same time. In most cases, the observed damage consisted in developing permanent deformations (with displacements that affected the entire structure or a portion of it) and, in some cases, the collapse of a part of the facing system.

The possible disadvantages limiting the use of these structures are represented exclusively by the request of sufficient space on the back of the facing for the reinforcements' installation, by the possible

difficulty of finding the granular materials when they are not available on site, and by the lack of regulatory support not always adequate to the needs of designers.

3. Geosynthetics for reinforced soil structures

Reinforcement function permits to improve the shear strength and deformation characteristics of soil by embedding inside of it a geosynthetic characterised by high tensile strength and stiffness, so that it is possible to build reinforced retaining walls or steep slopes even using low-strength soils.

Geosynthetics as reinforcing elements may be used: (i) to build reinforced earth retaining structures, bridge abutments, embankments and steep slopes; (ii) as basal reinforcement beneath embankments over soft foundation soil (even in presence of piles); (iii) to realize geosynthetic-encased columns (GEC) in soft soil; (iv) to build passive structural barriers for landslide risk mitigation [KOFFLER *et al.,* 2008; BRANDL, 2011]; (v) to prevent localised sinkholes; (vi) to realise waterways and flood protection structures; (vii) to reinforce barrier systems of landfills [ZORNBERG and KAVAZANJIAN JR, 2001; PALMEIRA *et al.,* 2008; TOUZE-FOLTZ *et al.,* 2016]; (viii) to reduce the seismic thrust acting on rigid retaining structures; (ix) to improve foundation soils; (x) to stabilise roadway or railway foundations and reduce pavement cracking [PERKINS and ISMEIK, 1997a; PERKINS and ISMEIK, 1997b; PERKINS, 1999; KWON e*t al.,* 2005; YANG and AL-QUADI, 2007; WU *et al.,* 2015; CORREIA and ZORNBERG, 2016].

3.1. General overview

Use of geosynthetics as basal reinforcement of earth embankments on soft foundation soils allows eliminating the overall stability problems related to the weight of the embankment by preventing shear failure both in the embankment fill (rotational stability and lateral sliding stability of the embankment fill) and in the foundation soil (foundation extrusion stability).

Geosynthetics can be used also as basal reinforcement of piled embankments (or other columnar treatments) in highly compressible soil. In this case, the presence of the geosynthetic allows increasing the load rate transmitted to the pile foundations and the horizontal spacing between the piles, and avoiding the use of inclined piles near the edge of the embankment since the active thrust force weighs on the geosynthetic.

The use of geosynthetics to reinforce sand and gravel columns provides a cheaper alternative to the use of pile foundations. Geosynthetics allow the construction of reinforced gravel and sand columns (Geosynthetic encased columns-GEC) even in the presence of soft cohesive soils ($c_u < 15$ kN/m^2) which could not guarantee sufficient lateral support for the construction of traditional gravel or sand columns.

Geosynthetic-reinforced embankments are used increasingly as passive structural barriers against landslides (rock falls, avalanches, mud/debris flows, etc.) and coastal protection measures. In these applications, geosynthetics allow spreading the impact energy on a greater surface, consequently reducing stress and strain state in the embankment body.

Geosynthetics are widely used as reinforcement, separation, filtration, sealing and drainage to stabilise paved and unpaved roadways improving their performance (also when they are founded on problematic soils as expansive clay subgrades) during construction or restoration works. Literature shows clear evidence that stabilisation provided by geosynthetics improves the pavement service life and permits equivalent pavement performance with a reduced structural section (reducing costs). Nevertheless, no unanimous scientific consent on the actual mechanisms governing the pavements reinforcement can be found yet since they are still largely unmeasured.

The "membrane effect" in the reinforcing geosynthetic can be used to construct road and railway platforms in areas with localised sinkholes. In these cases, the deformed geosynthetic sustains normal and shear stresses providing a support (by means of the vertical component of the membrane's force) to the overlying soil mass subjected to loading [GIROUD and NOIRAY, 1981; BOURDEAU *et al.,* 1982; LOVE *et al.,* 1987; MADHAV and POOROOSHASB, 1988; BOURDEAU, 1989; SHUKLA and CHANDRA, 1994].

Geosynthetics can be used with reinforcement function to ensure stability of landfill cover systems and to reduce the tensile stress state acting on the geomembranes of the perimeter barrier systems (veneer stability).

Finally, the most common applications of geosynthetics in this field are those which allow reinforcing steep slopes and building retaining walls. Since these applications are the main subject of the current paper, they will be debated more in detail in the following sections.

3.2. Steep slopes and retaining walls: constructive techniques and filling soils

The distinction between retaining walls and steep slopes when reinforced with geosynthetics is of a conventional nature, being it typically related to some traditional analysis and design procedures. Generally, the term *wall* is used when the external facing of the structure is vertical or sub-vertical

(characterised by an angle β with respect to the horizontal above 70°); instead, the term *steep slope* is reserved for cases in which $\beta \leq 70°$.

With regard to the soil constituting the reinforced block, the international recommendations [BS 8006, 2010; EBGEO, 2010; FHWA-NHI, 2009; RTRI, 2007, etc.] suggest the use of granular soils in the first instance; other types of soil can be used with strict restrictions and demands related to the internal drainage of the work.

In order to extend effectively the use of reinforcement technology with geosynthetics also to cohesive filling soils, several researches have been carried out [O'KELLY and NAUGHTON, 2008; ZORNBERG and KANG, 2005; ABDI and ARJOMAND, 2011; KANG *et al.*, 2015; THUO *et al.*, 2015]. The aim of the aforementioned studies is to develop new materials (essentially geocomposites for reinforcement and drainage) or new technical solutions (geogrid insertion in small sand layers). However, these technologies do not appear to be fully mature yet and further researches are needed for their development and safe use.

The filling soil, the foundation soil and the soil behind the reinforced structure must be characterised by means of in-situ or laboratory tests to determine their physical, chemical and geotechnical parameters. It is recommended to perform tests for identification [ASTM D2488, 2017], tests for determining soil shear strength (direct shear tests, triaxial tests, plane strain tests), compaction tests [AASHTO T 99, 2015; AASHTO T 180, 2015], tests that allow establishing the potential soil aggressivity towards the polymer constituting the reinforcement, such as those necessary to determine pH [AASHTO T289, 1991; ASTM D4972, 2019], electrical resistivity and salt content [AASHTO T290-95, 2016; ASTM D4327, 2017].

The methods used for the construction of geosynthetic-reinforced soil structures can be classified essentially according to the type of solution adopted for the facing and the type of connection between the facing and the reinforcement elements (when the facing is present). The facing system can be built wrapping the geosynthetic around or using precast concrete panels or rigid blocks connected to the geosynthetic (SRW-Segmental Retaining Wall), gabions, projected concrete, wooden panels, cellular polymeric containment systems [FHWA-NHI, 2009], cast-in-situ (Full Height Rigid, Japanese National Railway).

The wrap-around technique, widespread since the early 1980s, can be used to create both retaining structures with vertical facing and steep slopes. For the latter, the use of a flexible facing is the most widely used design solution. The construction procedure involves the use of permanent formworks, consisting of electro-galvanised welded wire meshes with square opening bent to the desired facing angle, staked to the ground and connected to one another. Thereafter, a geosynthetic is cut according to the design length and laid on the ground and on the formwork. An overlapping between two adjacent reinforcement layers must be provided: for instance, the American recommendations FHWA-NHI [2009] establish a minimum overlapping of 150 mm; alternatively, they suggest connecting the side edges to each other when geogrids are used. To avoid soil coming out during the compaction phase and to facilitate slope's facing planting greenery, a geomat coupled with a pre-seeded vegetative biofelt can be used with appropriately selected species (possibly native ones) depending on the environment and climate; for this purpose, vegetable soil is used near the facing system. Subsequently, the permanent formwork stiffens by means of spaced metal tie rods in order to prevent facing's deformations during the compaction phase. At this point it is possible to proceed with the placement of the soil layer, which must be well compacted. A light compactor should be used carefully near the facing or workmen could even proceed manually.

Compaction must be carried out until reaching a dry unit weight of at least 95% of the maximum dry unit weight obtained by AASHTO T 99 [2015] Standard Proctor compaction test [ASTM D698, 2012; UNI EN ISO 13286-2, 2010], using compactors of adequate energy and adding the water needed to optimise the procedure. In Japan, the current technical standards, particularly attentive to the compaction phase, recommend reaching a dry unit weight of approximately the 95% of the maximum unit weight obtained by AASHTO T 180 [2015] Modified Proctor test [ASTM D1557, 2012]. To obtain the expected result, it is essential to compact layers of soil not exceeding 15-30 cm. Since it is not possible to reproduce the energy conditions of the laboratory compaction in situ, the compaction achieved with a mechanical equipment (static rollers, vibratory and impact compactors, etc.) must be verified in field by a serious control program (verification of the dry design density), that is by using destructive [ASTM D1556, 2015; ASTM D2167, 2015] or non-destructive techniques [ASTM D 6938, 2017].

The construction of the compacted soil layers continues until reaching the design vertical spacing between geosynthetic layers (distance between two consecutive reinforcement levels). The geogrid that had been placed temporarily on the permanent formwork is wrapped around the soil layer, repeating the procedure layer-by-layer until the work is completed. The aforementioned specifications concerning the soil compaction remain valid for all the construction methods, such as those involving the use of concrete panels or blocks on the facing connected to geosynthetics.

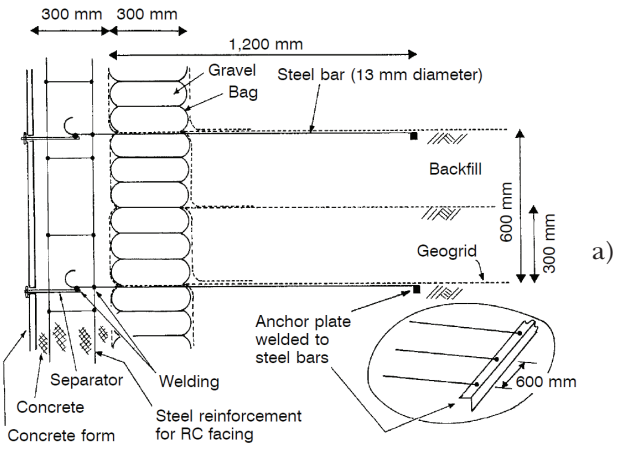

a)

b)

Fig. 1 – a) Construction scheme of reinforced earth walls with rigid facing (GRS RW-FHR) developed in Japan; b) detail of the connections between the facing and the reinforced block [modified from TATSUOKA, 2008].
Fig. 1 - a) Schema costruttivo di un muro in terra rinforzata con facciata rigida (GRS RW-FHR); b) particolare delle connessioni tra la facciata e il blocco rinforzato [modificato da TATSUOKA, 2008].

For very high structures, the use of facing configurations with berms or slope inclinations varying with height (for example bi-linear profiles) allows a reduction of the tensile load acting on reinforcements compared to the configuration with constant inclination of the facing.

The use of panels or blocks is very common worldwide and is generally used for the construction of retaining walls and bridge abutments. In Europe, prefabricated concrete blocks [BS 8006, 2010] must comply with some technical requirements (compressive strength, imbibition, density, cement content and water-cement ratio) and should follow BS EN 771-3 [2011] and BS EN 12878 [2014] Standards.

Following the Kobe earthquake in 1995, a reinforced earth wall construction procedure was developed in Japan, capable of guaranteeing a great performance with zero (or very small) time of rail or road service resumption after major seismic events. This technology, called GRS RW-FHR (Full Height Rigid), is characterised by a continuous rigid facing that is built after the construction of the reinforced soil block to which the rigid facing is strongly connected. The Japanese National Railway has promoted this construction technique as standard for the building of new retaining walls or embankments and the reconstruction of those damaged during seismic or alluvial events [TATSUOKA *et al.*, 1997; TATSUOKA *et al.*, 2007]. The GRS RW-FHR technology consists of the following phases: 1) levelling of the soil foundation and construction of the generally small foundation structure of the facing; 2) placement of the reinforcing geosynthetic and the gabion filled with gravel, which constitutes the formwork for the wrap-around facing; 3) compaction of a soil layer by using high compaction energy; 4) realisation of the next reinforced layers until reaching the height needed; 5) construction of a rigid cast-in-place reinforced concrete facing having generally a small thickness (FHR) when reinforced block and soil foundation settlements ran out. During this phase, using reinforcing steel bars (connected to the geosynthetics) previously inserted in the reinforced block ensures a strong connection between facing and the reinforced soil block (Fig. 1).

By considering only GRS RW-FHR works made in Japan in the 1989-2014 period, a longitudinal extension exceeding 158 km can be highlighted [YONEZAWA *et al.*, 2014]. Compared to the traditional cantilever walls, GRS RW-FHR technology avoids concentrations of tensions at the wall toe, which could require the use of pile foundations. Unlike the case where the facing is flexible or the reinforcement layers are not connected to a stiff facing, in the GRS RW-FHR technology the presence of a strong connection on the facing even allows it to be subject to tensile load actions similar to those occurring at the failure surface. This circumstance implies that the soil delimited by the failure surface is subject to high confinement tensions that increase its strength and stiffness, thus improving its mechanical behaviour compared to the case where the facing connection is absent, especially in seismic conditions (Fig. 2).

With regard to the facing-reinforcement connections, a designing key point is to estimate the action value, *i.e.* the tensile load acting on the geosynthetic layer. By using the classic tieback wedge method the maximum tensile load required for the reinforcement, which is mobilised at the limit of separation between the active and the resistant zone of the reinforced block, can be calculated easily. The more flexible the adopted facing system, the lesser the tensile load acting at the facing connection. For any limit state, FHWA-NHI [2009] recommends the connec-

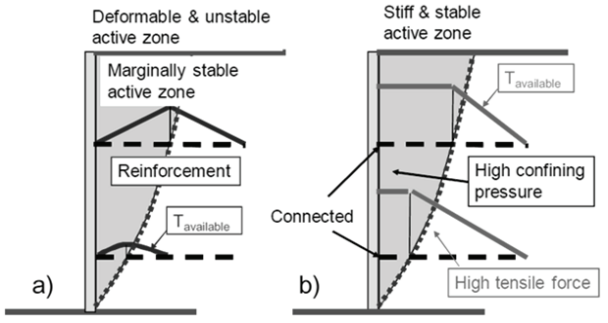

Fig. 2 – Effect of a strong connection between geosynthetic and facing [modified from TATSUOKA, 2008].
Fig. 2 – Effetto della forte connessione tra geosintetico e facciata [modificato da TATSUOKA, 2008].

tion to be designed considering the maximum tensile load. A conflicting approach regarding the way to operate can be observed in the various European recommendations. In particular, for the specific case of flexible facing, BS 8006 [2010] suggests to adopt a value equal to the 75% of the maximum tensile load at the top of the structure, which should be increased linearly with increasing depth, while EBGEO [2010] reduces it (50-70% of the maximum tensile load) in correspondence with the bottom part (from 0.4 H to H). This is linked to experimental results that are often conflicting, and difficult to read and predict. A reasonable and cautious assumption appears to be to consider the calculated maximum tensile load value. Moreover, it is necessary to underline how the resistance of the connections cannot be predicted in the absence of full-scale tests.

4. Advancement in soil reinforcement with geosynthetics

A correct design of GRS retaining walls or steep slopes must ensure margins of safety, which are fitting against the possible ultimate and serviceability limit states for both the structure and ground-structure, in accordance with regulations or guidelines in force.

The possible ultimate limit states to be taken into account for reinforced soil structures are the external stability limit states (such as sliding on the base, overturning, bearing resistance, overall stability), which can be analysed with the approaches usually adopted in Geotechnical Engineering for these kind of structures; the internal stability limit states (by failure of the reinforcements, either due to insufficient structural tensile strength or due to insufficient interaction resistance between soil and the reinforcements, and by failure of the facing, either due to insufficient strength of the facing or due to insufficient strength of the reinforcement connections); and the compound stability limit state (with a large slip mechanism that intercepts both the reinforced block and the back retained soil).

Serviceability limit states, which occur when the in-service deformation exceeds prescribed limits, can be referred to external (foundation settlements) or internal factors (reinforced mass deformations due to creep strain of polymeric reinforcements, creep of fine grained fill soil, presence of a layer of wet fill, polymer's degradation).

The analysis of possible internal instability mechanisms allows determining the tensile strength and stiffness of reinforcements, their spacing and anchorage length, and the structural characteristics of facing and connections. The starting point in designing GRS structures, which differentiates them from any traditional retaining work, is evaluating the tensile forces acting on the reinforcement levels. Experimental measurements carried out on full scale tests of geosynthetic-reinforced retaining walls have allowed both highlighting the trend of the maximum tensile forces along the geosynthetic specimens under serviceability conditions, and evaluating their evolution up to the moment where failure occurs. The emerged result is that the tensile curve's trend along the reinforcement remains practically unchanged when the load approaches the failure conditions, while the stress values in the individual bars increase. Failure occurs by the formation of a sliding surface in the reinforced soil mass; the sliding surface is approximately coincident with the locus of points of the maximum tensile load. The maximum tensile force acting on a generic reinforcement in the separation section between the active zone and the resistant (passive) zone works as a pullout load for the geosynthetic portion anchored to the resistant zone. Therefore, it is essential to check this value to be compatible with the design pullout resistance $P_{R,d}$ and the design resistance of the connections (when present), in addition to not exceed the design tensile strength $R_{t,d}$.

In light of what has been said up to this point, it is important to highlight that a detailed knowledge of the mechanical, chemical, physical characteristics and durability of geosynthetics, as well as of the interaction arising at the soil-geosynthetic interface, is required in order to design GRS structures correctly. Over the years, advances in knowledge about these topics have been collected, as shown in the following.

4.1. Geosynthetics used for reinforcement and their constituent polymers

4.1.1. PROPERTIES AND DURABILITY

The synthetic polymers generally used to produce geosynthetics working with reinforcement function are mainly polypropylene (PP), high-den-

Tab. I – Mechanical characteristics of commercially available reinforcing geosynthetics.
Tab. I – Caratteristiche meccaniche dei geosintetici di rinforzo disponibili in commercio.

Polymer	Type of product	T_F (kN/m)	ε_F (%)
PET	Knitted Geogrids	20 – 1200	8 - 15
	Welded Geogrids	20 – 500	6 - 10
	Woven Geotextiles	100 – 1600	8 - 15
HDPE	Knitted Geogrids	20 – 300	15 - 20
	Extruded Geogrids	40 – 200	10 -15
	Woven Geotextiles	30 – 400	15 - 20
PP	Knitted Geogrids	20 – 500	8 - 15
	Welded Geogrids	20 – 400	8 - 15
	Extruded Geogrids	20 – 50	8 - 20
	Woven Geotextiles	20 – 600	8 - 20
PAr	Knitted Geogrid	40 – 2200	2 - 4
	Woven Geotextiles	10 – 2400	2 - 4
PVA	Knitted Geogrid	30 – 1600	4 - 5
	Woven Geotextiles	30 – 1800	4 - 5

sity polyethylene (HDPE), polyamide (PA) and polyester (PET). For specific applications, geosynthetics produced with polymeric materials made with extremely high strength fibres (Aramids – Ar) can be used. Reinforcements that are even suitable to be used with cohesive soils stabilised with lime (characterised by very high pH values) or to be used in contact with concrete are realised through the polyvinyl alcohol (PVA) [AYDOGMUS *et al.*, 2007; TATSUOKA, 2008].

The polymeric fibres have a semi-crystalline structure made of polymers, which is partly made up of perfectly oriented chains (crystalline part) and partly of chains arranged randomly (amorphous part). The rupture can be governed either by the breaking of chemical bonds (very rarely) or by stretching and separation between the chains when the cohesive (intermolecular) forces are exceeded. Creep sensitivity under tensile loads depends on both the tensile loading level and the operating temperature. Glass transition temperature (T_g) is the temperature at which the amorphous polymer changes from a glass to a rubbery state; this temperature is the macro-manifestation of polymer chain's flexibility. The difference in behaviour between polymers is essentially due to the fact that the ambient temperature T is lower or higher than the glass transition temperature. For instance, in the case of PET the ambient temperature is lower than T_g, while it is higher for polyolefins (PP, PE). When $T>T_g$ the polymers behave like "rubbery" materials (visco-plastic behaviour prevails).

The degree of crystallinity depends on the polymer's type and structure and on the growth conditions: when an adjacent monomer molecule reacts with an active site of the monomer, chain addition is said to have occurred [BHAT and KANDAGOR, 2014]. Narrow molecular weight, linear polymer chains, and high molecular weight increase the crystallinity, which is affected also by extrinsic factors, like crystallization temperature, cooling rate and, in the case of strain-induced crystallization, by the stretch ratio, strain rate, and by the forming process of the polymer film or fibre. Crystallization can be induced also by stretching a polymer; in this case, crystallization is caused by molecular orientation in the stretch direction. Therefore, properties of the polymeric fibres, which mainly influence the long-term behaviour of the polymer, can be improved in the production phase by varying the molecular weight of the constituents or by orienting the molecules by means of an industrial stretching process (which produces an increase in the degree of polymer's crystallinity).

In addition to the degree of crystallinity, the chemical-physical and mechanical (short and long term) characteristics of the polymers commonly used in civil and environmental engineering mainly depend even on molecular orientation and intermolecular cohesion forces acting between the constituent chains [COOKE and REBENFELD, 1988]. Specific attention must be paid to the in-field conditions in choosing the polymer, since the pH of the soils in contact, the oxidizing agents and the UV rays must be taken into account.

The first geosynthetics being produced were geotextiles; in particular, the first industrial productions of short fibre non-woven geotextiles were manufactured in Italy and France in 1958, while the first example of using polymeric materials for the construction of a reinforced soil wall dates back to 1972 in United Kingdom. In this application, the reinforcing elements consisted of continuous glass fibres inserted inside a protective resin coating.

Nowadays, the most used geosynthetics with reinforcement function are geogrids and woven geotextiles. Woven geotextiles (GTXw) are manufactured by using several types of yarns [SHUKLA, 2016], such as *monofilament yarn* (single filament), *multifilament yarn* (filaments aligned together), spun yarn (interlaced or twisted staple fibres), *slit film yarn* and *fibrillated yarn* (made of strands). The yarns cross to form fabric in the warp and weft directions. Geogrids (GGR) are flat structures that look like open mesh grids (openings > 6.35 mm), and can be extruded, woven or with welded strips. The production of extruded geogrids made of HDPE or PP occurs by means of an extrusion process and subsequent stretching in one or two directions. Woven geogrids are generally made of PET fibres covered with a protective layer, also made of synthetic material, able to guarantee the structural strength of the joints. They can be manufactured also using PVA and Ar

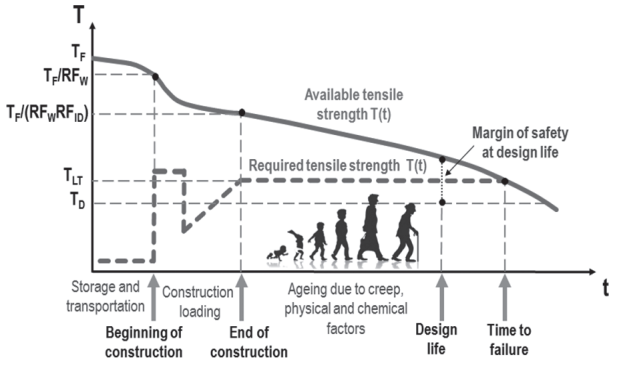

Fig. 3 – Available and required tensile strength of a geosynthetic during storage and transportation, installation and construction, and use of the structure over time (modified from ISO/TS 13434, 2008).

Fig. 3 – Resistenza a trazione di un geosintetico richiesta e disponibile durante le fasi temporali di immagazzinamento e trasporto, installazione, costruzione ed esercizio (modificato da ISO/TS 13434, 2008).

fibres. Geogrids with welded strips consist of two or more series of fibres connected at regular intervals by welding; they generally have a core of high tenacity PET filaments and a PE coating. The first oriented extruded polymeric geogrids were manufactured in England in the 1970s and the first use of polymeric geogrids dates back to the construction of a reinforced soil wall built in a Yorkshire (UK) railway station in 1979.

Tab. I lists the short-term ultimate tensile strength, T_F, and the corresponding tensile strain, ε_F, of commercially available products. It is possible to notice the great variety of products, with tensile resistances and tensile strains ranging from 10 kN/m to 2400 kN/m and from 2% to 20% respectively, thus entailing a large field of possible applications.

The design of geosynthetic-reinforced soil structures based on limit equilibrium or kinematic hybrid methods requires the knowledge of both the long-term tensile strength of the geosynthetic and the parameters representative of the behaviour at the soil-reinforcement interface. With regard to the first point, it is necessary to introduce the concept of durability, which can be defined as the geosynthetic's capability to maintain the required mechanical characteristics for all the design working life, preventing the occurrence of possible ultimate and serviceability limit states. Therefore, the long-term tensile strength is the value of the tensile load that causes the geosynthetic's tensile failure if applied for the entire design working life of the structure. Long-term tensile strength must take into account all the possible reductions in resistance that occur during the construction or serviceability phase due to mechanical, physical, chemical, and environmental degradation, or those related to the visco-elasto-plastic nature of the constituent polymers (creep effects). The approach commonly followed by the various international recommendations is to calculate the long-term tensile strength value by dividing the short-term tensile strength to safety reduction factors taking into account the aforementioned effects.

The characterisation of the short-term mechanical behaviour of geosynthetics (*i.e.* the short-term ultimate tensile strength T_F, among other things) can be carried out following standard test procedures [UNI EN ISO 10319, 2015; ASTM D6637, 2015] for the execution of wide-width tensile tests on geosynthetics tested in air. In addition, in the case of geogrids the junctions must be tested appropriately [ASTM D 7737, 2015]. According to UNI EN ISO 10319 [2015], wide-width tensile tests under monotonic loading must be carried out on a number of five representative specimens in the standard atmosphere for testing (20 ± 2°C at 65 + 5% RH), as defined by ISO 554 [1976]. Each specimen must be clasped with special clamps that prevent internal movements; during the test, the clamps advance at a fixed displacement rate so that to guarantee a constant specimen strain rate (equal to 20% per minute).

Tensile strength of polymeric materials (polyolefins above all) is strongly affected by the adopted testing rate; specifically, it increases highly with increasing test rate due to their characteristic viscous behaviour. For this reason, the Japanese test method [PWRC, 2013] recommends the adoption of a testing rate so that to guarantee a strain rate equal to 1% per minute [MIYATA *et al.*, 2014], while the American standard [ASTM D6637, 2015] suggests a strain rate equal to 10% per minute. This circumstance means that the reduction factors listed in the different design recommendations must be applied to short-term tensile strengths that have been measured by following the Standard suggested by the same recommendation the designer is using.

Referring to ISO/TR 20432 [2007], the reduction factors are representative of creep under static tensile loads (RF_{CR}), mechanical damage during installation (RF_{ID}), environmental effects (RF_W) and possible chemical and biological attacks (RF_{CH}). Moreover, the tensile strength is further reduced by using another reduction factor (FS) taking into account both the variability of material production and the procedures used to extrapolate the experimental data obtained by performing short-term durability tests to the design working life. Figure 3 summarises these concepts by plotting the development of both the available and required tensile strengths of a geosynthetic over time. Specifically, the graph shows the evolution of these parameters during the stages of storage and transportation, in-

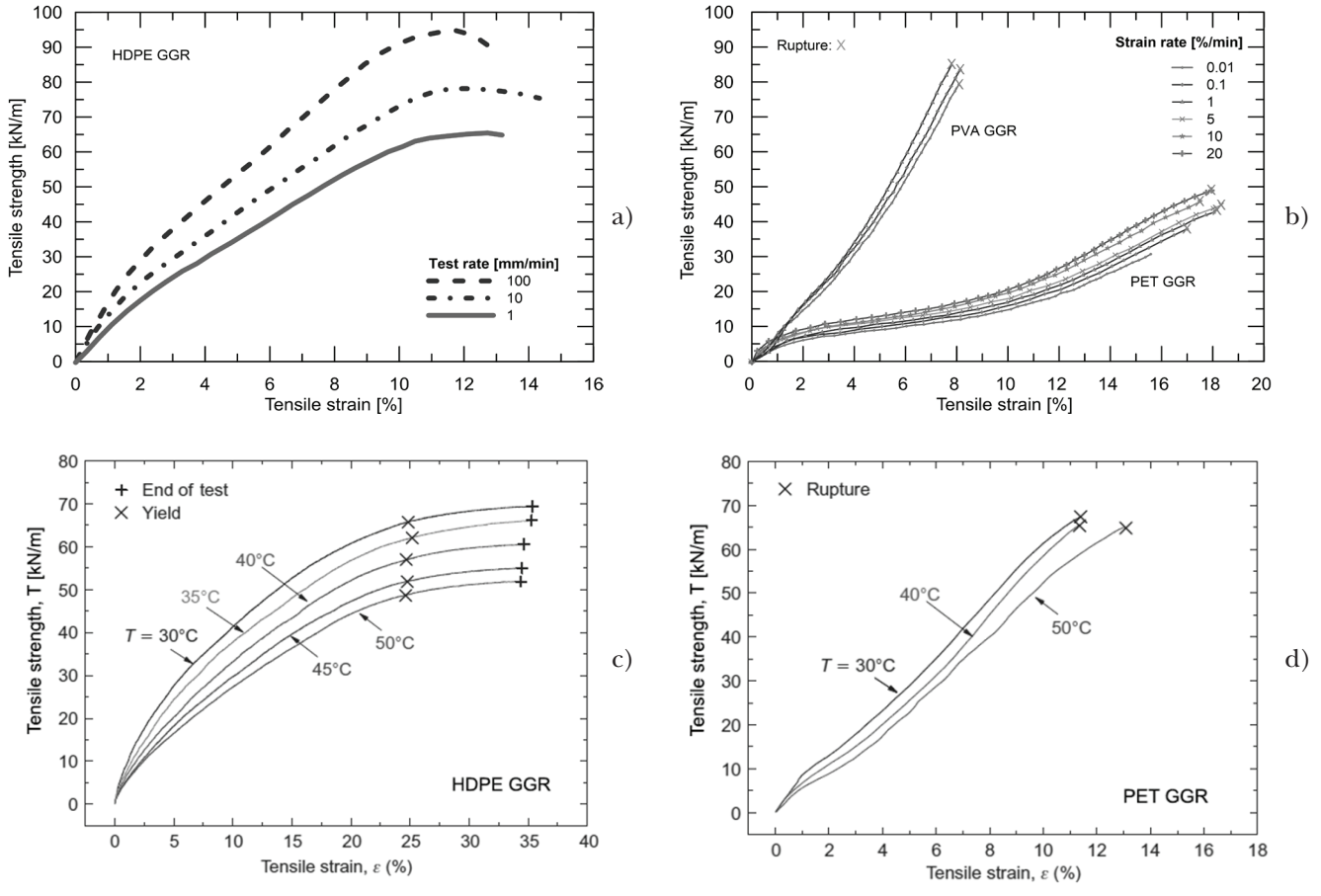

Fig. 4 – Stress-strain curves for different geogrids, resulting from monotonic tensile tests: influence of test rate a) on HDPE extruded geogrid, b) on PET and PVA woven geogrid and influence of temperature c) on HDPE geogrid, d) on PET geogrid [modified from KONGKITKUL *et al.*, 2012; MORACI, 2011].

Fig. 4 – Curve resistenza a trazione-deformazione ottenute da prove monotone di trazione condotte su differenti geogriglie: influenza della velocità di prova a) geogriglia estrusa in HDPE, b) geogriglia tessuta in PET e PVA; influenza della temperatura c) geogriglia in HDPE, d) geogriglia in PET [modificato da KONGKITKUL et al.*, 2012; MORACI, 2011].*

stallation and construction, use of the structure until reaching the design working life and the failure at a later time.

In order to calculate RF_{CR}, creep tests must be performed on specimens tested in-air (by applying a constant tensile load over time in the standard atmosphere for testing), while recording the time in which the applied load causes rupture. The tests must be carried out at least 12 times at different load levels and repeated at temperatures higher than the design one. The representative points of creep rupture are then normalised with respect to the short-term ultimate tensile resistance (T/T_F) and plotted in a semi-logarithmic graph (time being on a logarithmic scale) where they are fitted using statistical regression analysis; afterwards, the data referring to temperatures higher than the design temperature will be shifted according to the time-temperature shifting (TTS) method up to meeting the data envelope obtained at 20°C [ISO/TR 20432, 2007].

4.1.2. MECHANICAL BEHAVIOUR OF GEOSYNTHETICS SUBJECTED TO DIFFERENT TYPES OF LOAD

In order to analyse the mechanical behaviour of geosynthetics for soil reinforcement subjected to monotonic, sustained and cyclic loadings, different researches were carried out [BATHURST and CAI, 1994; MORACI and MONTANELLI, 1997; HIRAKAWA *et al.*, 2003; KONGKITKUL *et al.*, 2004; LIU and LING, 2006, 2007; TATSUOKA, 2008; CARDILE *et al.*, 2016b; CARDILE *et al.*, 2017b]. These studies also considered complex tensile loading conditions. Typical experimental results obtained in previous researches are summarised in the following.

Stress-strain curves obtained during monotonic tensile tests (carried out at constant strain rate) are non-linear. Depending on geosynthetic structure (*e.g.* woven or extruded geogrids) and constituent polymers, three different types of non-linearity can be defined. Specifically, the tensile stiffness decreases with increasing tensile strain for HDPE extruded

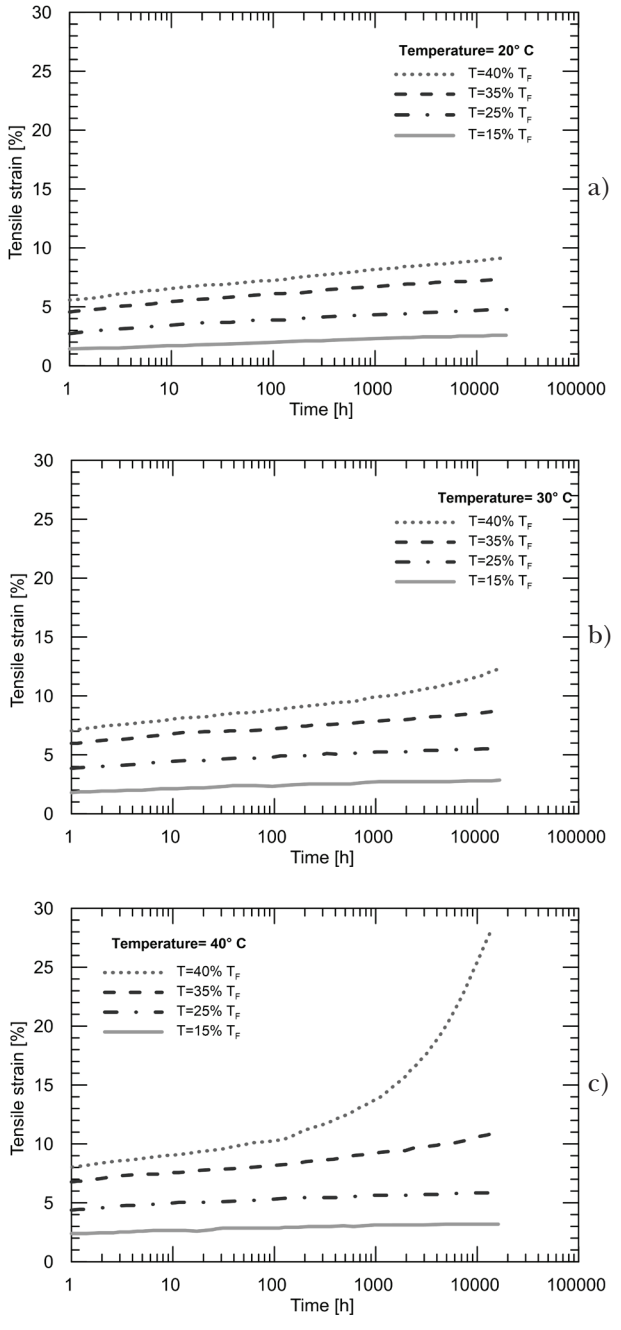

Fig. 5 – Tensile creep test results for HDPE extruded geogrids carried out at different temperature: a) 20°C; b) 30°C; and c) 40°C [MORACI and MONTANELLI, 1995].
Fig. 5 – Risultati di prove di trazione condotte su geogriglie estruse in HDPE a differenti temperature: a) 20°C; b) 30°C; e c) 40°C [MORACI e MONTANELLI, 1995].

geogrids (Fig. 4a), while it increases for PVA woven geogrids; for PET woven geogrids the tensile stiffness first decreases and then increases with increasing tensile strain, as it can be observed in figure 4b. Figures 4a,b even show the loading rate influence on the tensile strength values, which increase with increasing it. On the contrary, the tensile strength decreases with increasing service temperature (thus highlighting the viscous behaviour of these types of materials). These effects are more accentuated for PP and HDPE geosynthetics, while are smaller for PET materials (Figs. 4c,d).

With regard to the creep behaviour, results obtained by tensile creep tests, carried out on HDPE extruded geogrids at different temperatures (20°C, 30°C and 40°C) by using loads chosen as a percentage (15%, 25%, 35% and 40%) of the short-term ultimate tensile strength (T_F), showed that the creep strains increase with increasing applied tensile load and temperature (Fig. 5). For temperature equal to 20°C, the curves show a linear behaviour in a semi-logarithmic graph within the testing period (2 years), regardless of the applied load, while for higher temperatures (40°C) a typical tertiary creep curve can be observed, which led to the specimen rupture. The tensile creep effects are instead more restrained in the case of PET geogrids, and they depend only on the applied load.

During the working life of the structure, geogrids can be subjected not only to static tensile loads that are constant over time (essentially due to the structure's self-weight and other sustained loads), but also to cyclic or dynamic loads (long-term cyclic vehicular loads or short-term seismic loads).

Under cyclic tensile loading, the development of a hysteresis load-strain behaviour as well as residual strains caused by cyclic loading is highlighted. To this end, CARDILE *et al.* [2016b; 2017b] studied the cyclic and post-cyclic tensile behaviour of an HDPE extruded uniaxial geogrid by means of several monotonic and multi-stage wide-width tensile tests. The authors used a multi-stage tensile test procedure (Fig. 6), which consists of three stages. The first one is a pre-stress stage representative of serviceability conditions, which retraces the reference monotonic curve at a constant strain rate (CSR) equal to $\varepsilon' = 0.2\%$ per minute, until reaching a fixed tensile monotonic load P_i (chosen as a percentage of T_{max}, that is the maximum tensile strength per unit width

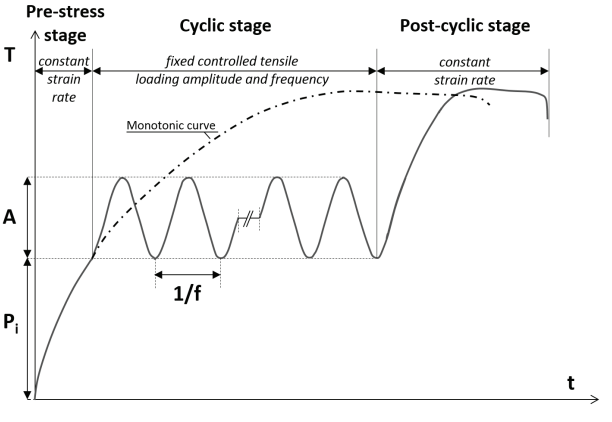

Fig. 6 – Multi-stage procedure [CARDILE *et al.*, 2017b].
Fig. 6 – Procedura multi-stage [CARDILE et al., 2017b].

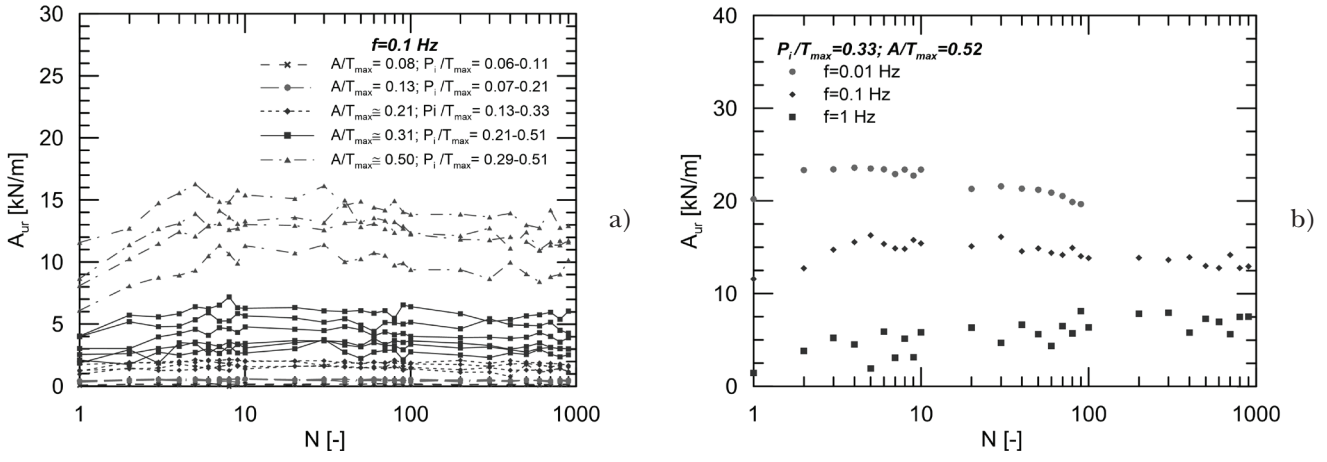

Fig. 7 – Hysteretic area with varying numbers of loading cycles, for tests performed at a) f = 0.1 Hz and b) for tests at different frequencies [modified from CARDILE *et al.*, 2017b].

Fig. 7 – Area dei cicli d'isteresi al variare del numero di cicli, per prove condotte a a) f = 0.1 Hz e b) per prove condotte a differenti frequenze [modificato da CARDILE et al., *2017b].*

obtained by monotonic test carried out at the same strain rate). The second stage is a load-controlled cyclic stage obtained by using a sinusoidal function, with fixed tensile loading amplitude *A* (chosen as a percentage of T_{max} as well) frequency *f* and number of cycles *N* (characterising a specific cyclic loading history). Finally, the last stage is a monotonic stage once again (at the same CSR of the first stage) useful to verify the influence of the applied cyclic loading on geogrid's tensile strength. In the above-mentioned research, the effect of cyclic tensile loading histories on those parameters that are characteristic of hysteresis loops (*i.e.* the maximum and residual strains cumulated during each cyclic loading, tensile stiffness and area of the hysteresis loops) were investigated. The hysteretic area A_{ur} included in the hysteresis loops depends on both loading amplitude and frequency. In particular, it remains almost constant over all loading cycles when the loading amplitude is low; by contrast, when the loading amplitude increases, A_{ur} increases for the first ten loading cycles and then decreases (Fig. 7a). The hysteretic area also increases with decreasing frequency (Fig. 7b). Moreover, figure 8 shows that the cyclic loading history does not induce a reduction of the tensile strength in the material (in the range of the investigated values). Actually, a very small increase in strength with increasing loading amplitude *A* can be observed; this behaviour could be explained by reference to the increased strain rate during cyclic stages carried out at the same frequency. However, these differences appear to be insignificant and comparable with the production variability of the materials, as they are always positive and lower than 6%. The same research developed and proposed a combined empirical model that is capable to predict, in the range of the investigated values, the geogrid's tensile behaviour under cyclic loading conditions, providing an expression for modelling the reinforcements' damping when performing numerical analyses of GRS structures.

However, it is important to highlight that the above considerations, which lead to the formulation of elastic-viscous-plastic constitutive models for the mechanical behaviour of geosynthetics [HIRAKAWA *et al.*, 2003; KONGKITKUL *et al.*, 2004; LIU and LING, 2006, 2007; PENG *et al.*, 2010] are valid in absence of confinement and other deteriorating agents (*i.e.* chemical, physical, mechanical and biological agents) that should be introduced in the geosynthetics constitutive models.

4.2. Soil-geosynthetic interaction

The knowledge of soil-reinforcement interaction parameters and their evolution over time, also related to the variation of the applied loads, is particularly important for designing geosynthetic reinforced soil structures. In fact, the reinforcement length and, consequently, the size of the reinforced soil mass depend on the apparent coefficient of friction that is chosen to represent the soil-geosynthetic interaction.

Specifically, at the soil-geosynthetic interface three different elementary interaction mechanisms can be mobilised depending on the failure mechanism, soil grain size and structure of the reinforcement (continuous or open mesh-type): the skin friction between soil and the solid surface of the reinforcement (both in case of geotextiles and geogrids); the passive resistance mobilised against the elements placed transversely to the direction of the tensile load's application; and the skin friction aris-

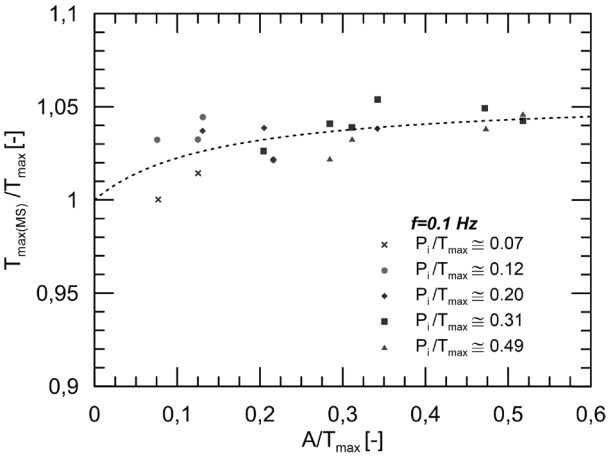

Fig. 8 – Ratio of maximum tensile strength obtained by multi-stage tests to that obtained by monotonic tests for varying normalised loading amplitudes and for different ranges of normalised pre-stress loads at f = 0.1 Hz [CARDILE *et al.*, 2017b].

*Fig. 8 – Rapporto tra la resistenza a trazione massima ottenuta da prove multi-stage e quella ottenuta da prove monotone, al variare delle ampiezze di carico normalizzate e per differenti range di precarico normalizzati a f = 0.1 Hz [*CARDILE et al., *2017b].*

ing because of soil shearing over soil through the apertures [JEWELL *et al.*, 1985], the last two possible only on geogrids.

In recent years several theoretical and experimental studies have been developed, allowing the comprehension of the soil-geosynthetic interaction. Considering a geosynthetic-reinforced soil structure, the reinforcement's action is triggered through different soil-geosynthetic interaction mechanisms that develop when a specific failure mechanism occurs, such as:

– sliding of a reinforced soil portion along a soil-geosynthetic interface;
– pullout of reinforcement from the passive zone, that is the zone beyond the failure surface where the reinforcement is embedded and can provide bond.

Direct shear tests and pullout tests can simulate both mechanisms in laboratory by using large-scale apparatus.

Shear behaviour of soil-geosynthetic interface depends on several factors related to the stress state acting on soil-geosynthetic interface, type, geometry and stiffness of geosynthetics, soil grain size distribution, soil plasticity, soil density, moisture content, specimen size, drainage and loading conditions, displacement rate and magnitude, and other parameters [DIXON, 2010]. Its complex behaviour can be simplified by the introduction of an equivalent shear-stress distribution that allows evaluating an overall resistance.

The direct shear tests performed at the soil-geosynthetic interface are generally carried out according to BS EN ISO 12957-1 [2018] and ASTM D5321 [2019]. ASTM D5321 [2019] provides some tips on the minimum dimension of the shear box: greater than 300 mm (also suggested by other standards and different researches); 15 times the D_{85} value of the tested coarse soil; or a minimum of 5 times the maximum opening size (in plan) of the tested geo-

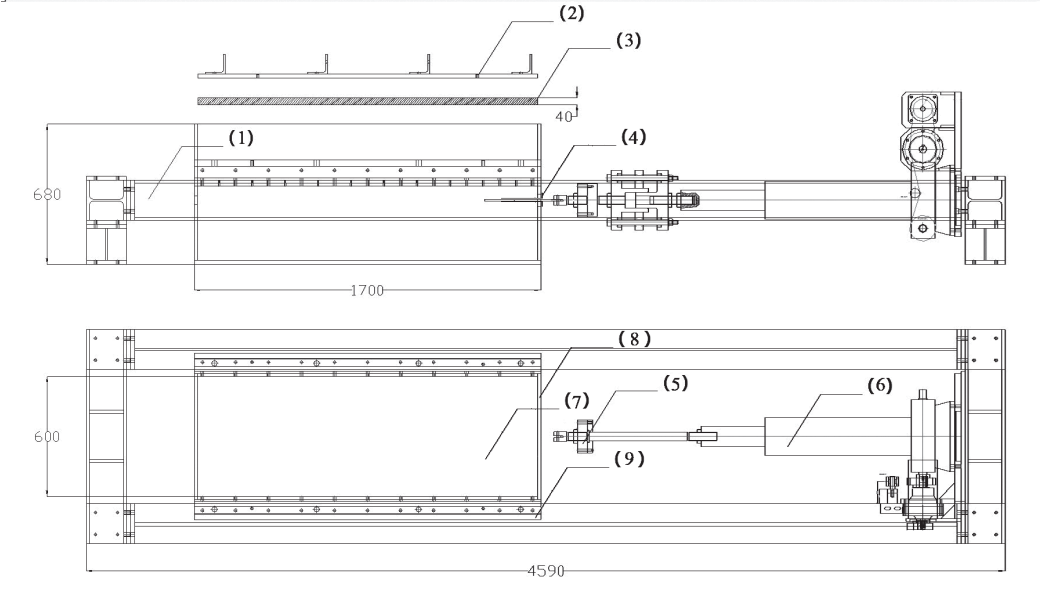

Fig. 9 – Scheme of pullout test apparatus [MORACI et al., 2017]: 1) frame; 2) steel plate; 3) air bag; 4) sleeves; 5) load cell; 6) hydraulic actuator; 7) 1700×600×680 mm pullout box; 8) front wall; 9) side wall.

Fig. 9 – Schema dell'apparecchiatura di sfilamento [MORACI et al., 2017]: 1) telaio; 2) piastra d'acciaio; 3) membrana flessibile; 4) angolari metallici; 5) cella di carico; 6) attuatore idraulico; 7) scatola di sfilamento 1700×600×680 mm; 8) parete frontale; 9) parete laterale.

synthetic. In addition, the depth of each shear box should be 50 mm or 6 times the maximum particle size of the tested coarse soil, whichever is greater. Referring to direct shear tests with geogrids, BS EN ISO 12957-1 [2018] suggests that the minimum dimensions of the boxes should be such that at least two full longitudinal ribs and three transverse bars are contained within the length of both upper and lower boxes.

Pullout tests allow studying the pullout interaction mechanism that develops in the anchorage zone at the soil-geosynthetic interface. Basically, pullout apparatus (Fig. 9) consists of a large pullout box made of rigid steel, a vertical load application system, a horizontal force application device, a clamp system and all the required measurement, control and data acquisition instruments [MORACI and MONTANELLI, 2000; MORACI and RECALCATI, 2006, MORACI *et al.*, 2017].

The test method is intended to be a performance test conducted as closely as possible to replicate design or as-built conditions [ASTM D6706-01, 2013]. Generally, pullout test procedure consists of the following steps: preparation of the internal walls; filling of the lower half of the pullout box with the chosen soil and its compaction; placement of the geosynthetic specimen and installation of test instrumentation along it; filling of the upper half of the pullout box and soil compaction; placement of the vertical load application system; closing of the pullout box; connection of the clamp system to the horizontal force application device; connection of test instrumentation; general setting and start of the test.

The various pullout test devices available worldwide differ in the box dimensions and methods used to minimise the boundary condition effects on test results. Moreover, different testing procedures are also used. In the last three decades different researchers carried out pullout tests using these different prototype apparatus in order to study the influence of boundary conditions and the scale effects of devices [PALMEIRA and MILLIGAN, 1989a; JOHNSTON and ROMSTAD, 1989; HAYASHI *et al.*, 1996; LOPES and LADEIRA, 1996; CHANG *et al.*, 2000; FARRAG and MORVANT, 2000; SCHMID and KAZDA, 2001; SUGIMOTO *et al.*, 2001; MORACI and RECALCATI, 2006; PALMEIRA, 2009]. The outcome of these studies allowed identifying the following factors affecting pullout test results: the influence of the vertical load application system; the influence of the boundary conditions at the front wall; the efficiency of methods used to minimise the friction between side walls and soil; the influence of the box sizes (specifically the thickness of soil below and above the geosynthetic specimen) to avoid boundary effects; the influence of geosynthetic specimen width compared to the pullout box width; the influence of the clamping device; the influence of the displacement rate used in the test. Based on the findings obtained by the researches on this topic, the following recommendations can be reassumed in order to define the characteristics that a pullout apparatus must have to ensure test results to be not affected by the above-mentioned factors:

- the vertical confining pressure should be applied by means of a flexible membrane;
- the side walls of the pullout box should be covered using low friction materials (*i.e.* Teflon, smooth aluminium, lubricated rubber membranes, etc.);
- sleeves (at least 200-300 mm long) should be used;
- an internal clamping system should be used so that the specimen is confined for the whole duration of the test;
- the soil height in the pullout box should be at least equal to 600 mm;
- the geosynthetic specimen width should be almost equal to the pullout box width;
- the pullout box sizes should be large enough to test a representative geosynthetic specimen.

In the following, the authors will focus on the analysis of soil-geosynthetic interaction under monotonic, cyclic and sustained loading conditions, specifically for the pullout limit state. The main conclusions drawn from different researches [CARDILE *et al.*, 2016a; CAZZUFFI *et al.*, 2011; MORACI and CARDILE, 2008, 2009a,b, 2012; MORACI and RECALCATI, 2006; CARDILE *et al.*, 2019; PISANO *et al.*, 2019] are discussed.

4.2.1. MODELLING THE SOIL-GEOGRID INTERFACE

With regard to the pullout limit state, the main interaction mechanisms mobilising the pullout resistance of geogrids embedded in a compacted soil are the skin friction between soil and the solid surface of reinforcement and the bearing resistance that develops against the transverse members [ZIEGLER and TIMMERS, 2004; MORACI and GIOFFRÈ, 2006; MORACI *et al.*, 2007; PALMEIRA, 2009; CALVARANO *et al.*, 2014; JACOBS *et al.*, 2014; MORACI *et al.*, 2014a]. Accordingly, the peak pullout resistance (P_R) of soil-geogrid interfaces has been typically modelled as the sum of these two above-mentioned components [JEWELL, 1996]:

$$P_R = P_{RS} + P_{RB} \tag{1}$$

where P_{RS} is the skin friction and P_{RB} is the bearing resistance. Generally, the two components are assumed to be independent from each other while in reality one interaction mechanism affects the other to an extent not yet well understood nor quantified.

The first term of equation (1) can be evaluated as follows [JEWELL, 1990]:

$$P_{RS} = 2\,\alpha_S\,L_R\,\tau = 2\,\alpha_S\,L_R\,\sigma_n'\,\tan\delta \tag{2}$$

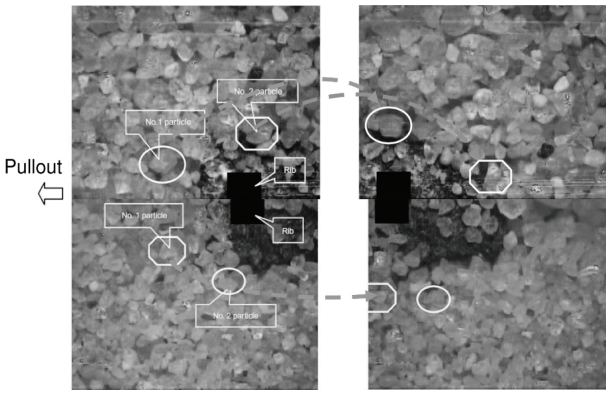

Fig. 10 – Particles motion around transverse rib: a) initial condition and b) subsequent position (modified from ZHOU *et al.*, 2012).

Fig. 10 – Moto delle particelle attorno ad una barra trasversale: a) fase iniziale e b) fase successiva (modificato da ZHOU et al., *2012).*

where L_R is the length of the geogrid in the anchorage zone, σ'_n is the effective stress acting perpendicularly on the interface plane; δ is the friction angle between soil and the geogrid; τ is the shear stress acting on soil-reinforcement interface; α_S is the fraction of the geogrid's surface where the friction mobilises actually (since the geogrid is open mesh-type).

The bearing component of the pullout resistance can be evaluated using the following expression:

$$P_{RB} = \left(\frac{L_R}{S}\right)\alpha_B \sigma'_b B \qquad (3)$$

where S is the spacing between the geogrid bearing members; L_R/S is the number of geogrid's bearing members; σ'_b is the effective bearing stress mobilising on geogrid's bearing members; α_B is the fraction of the geogrid's total transverse area where the bearing stress can act; and B is the thickness of the bearing members. To evaluate the bearing stress σ'_b, different failure mechanisms can be used. JEWELL *et al.* [1985] used a punching failure mechanism; PETERSON and ANDERSON [1980] used a general shear failure mechanism; BERGADO and CHAI [1994] used a modified punching mechanism; MATSUI *et al.* [1996] used a Prandtl failure mechanism. For granular soils, the bearing stresses σ'_b acting on geogrid's bearing ribs depend on soil shear strength angle, initial stress state, interface roughness and reinforcement depth in relation to the sizes of the bearing members. In spite of this, in the equations proposed by different authors the σ'_b/σ'_n ratio only depends on the soil shear strength angle.

Summarising, the pullout resistance of a soil-geogrid interface may be obtained as follows:

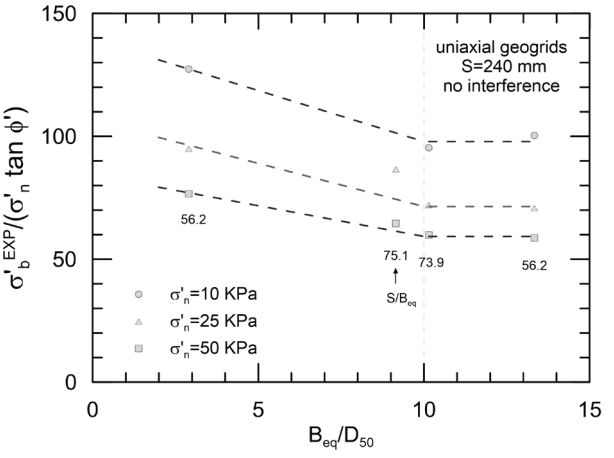

Fig. 11 – Scale effect: results of pullout tests in terms of $\sigma'_b/(\sigma'_n \tan\varphi')$ ratio, carried out on different soils using uniaxial geogrids in which interference effect is negligible [CARDILE *et al.*, 2017a].

Fig. 11 – Effetto scala: risultati delle prove di sfilamento, espressi in termini del rapporto $\sigma'_b/(\sigma'_n \tan\varphi')$ ratio, ottenuti su differenti terreni utilizzando geogriglie monoassiali in cui l'effetto interferenza è trascurabile [CARDILE et al., *2017a].*

$$P_R = 2\cdot\alpha_S\cdot L_R\cdot\sigma'_n\cdot\tan\delta + \left(\frac{L_R}{S}\right)\cdot\alpha_B\cdot B\cdot\sigma'_b = 2\cdot f_b\cdot L_R\cdot\sigma'_n\cdot\tan\varphi' \qquad (4)$$

where f_b is the interaction coefficient under pullout loading conditions; it can be obtained as function of reinforcement's geometrical parameters (α_S, α_B, B, S), soil shear strength angle (φ'), friction angle between soil and the geogrid (δ), and the stress state acting on the interface (σ'_n, σ'_b):

$$f_b = \alpha_S\cdot\left(\frac{\tan\delta}{\tan\varphi'}\right) + \left(\frac{\alpha_b\cdot B}{S}\right)\cdot\left(\frac{\sigma'_b}{\sigma'_n}\right)\cdot\frac{1}{2\cdot\tan\varphi'} \qquad (5)$$

The f_b value can be obtained also by back-analyses on pullout test results by using equation (4) in which the choice of the soil shear strength angle to be used is important and difficult. In order to avoid any assumption about the mobilised value, large-scale pullout tests allow determining the apparent coefficient of friction between soil and geosynthetic, $\mu_{S/GSY}$. The choice of using this design parameter is due to the fact that it depends on quantities that are known or easily measurable in laboratory:

$$\mu_{S/GSY} = f_b\cdot\tan\varphi' = \frac{P_R}{2\cdot L_R\cdot\sigma'_n} \qquad (6)$$

The mobilisation of the bearing resistance is strongly affected by the interference phenomenon for closely spaced bearing members (*i.e.* for a small value of the ratio between S and the thickness of transverse ribs B_{eq}). Actually, this phenomenon involves even a substantial part of the surface of the longitudinal members, entailing a decrease even in skin friction.

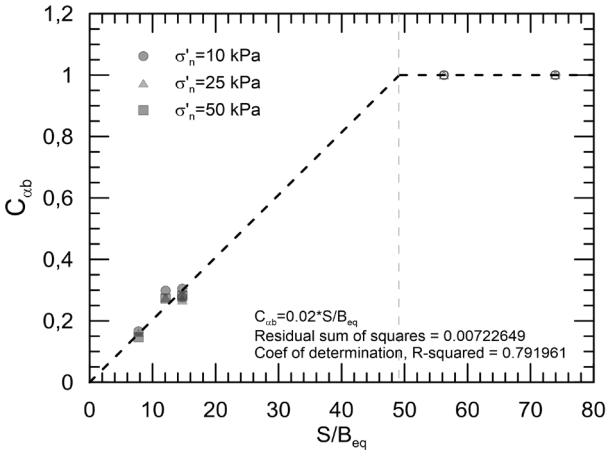

Fig. 12 – Variation of the reduction factor for the bearing resistance with varying normalised spacing between the transversal members [CARDILE *et al.*, 2017a].
Fig. 12 – Variazione del coefficiente riduttivo della resistenza passiva al variare della spaziatura tra le barre trasversali normalizzata [CARDILE et al., *2017a].*

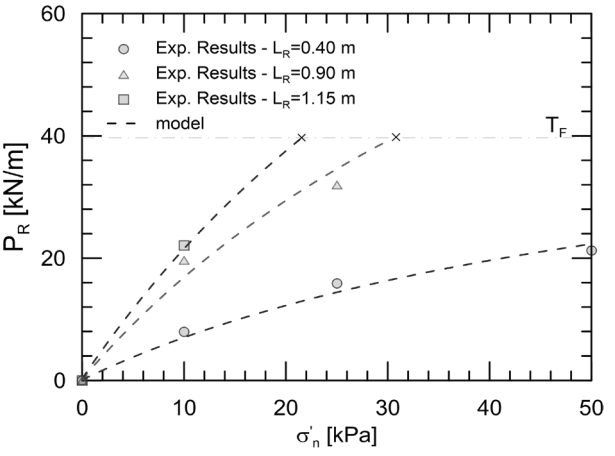

Fig. 13 – Comparison between experimental and theoretical values of peak pullout resistance for a biaxial geogrid embedded in a compacted uniform medium sand [modified from CARDILE *et al.*, 2017a].
Fig. 13 – Confronto tra valori teorici e sperimentali della resistenza allo sfilamento di picco per una geogriglia biassiale installata in una sabbia media uniforme compattata [modificato da CARDILE et al., *2017a].*

By using micro-image analysis, ZHOU *et al.* [2012] captured the interaction mechanisms between sand and the transverse ribs of the reinforcement, which was located close to the glass side walls. Figure 10 shows the particle motion around a transverse rib above and below the interface at various stages: sand particles located ahead of the transverse rib rotate during pullout; specifically, the particles above the geogrid's longitudinal axis rotate in clockwise direction while particles below rotate anticlockwise. Particles on the top right side of the transverse rib fall into voids created during the movement of the geogrid. The micro-image analysis confirms that the soil located in front of the transverse rib mobilises bearing stresses that are in the passive state, while a loose soil region is created and an active state is reached behind the transverse rib.

Bearing resistance also depends both on the ratio of the transverse rib's thickness B_{eq} to the soil average particle size D_{50} (*i.e.* scale effect) and on the shape of the transverse ribs [DYER, 1985; PALMEIRA and MILLIGAN, 1989b; MILLIGAN *et al.*, 1990; BERGADO *et al.*, 1993; JEWELL, 1996; PALMEIRA, 2004; 2009].

CARDILE *et al.* [2017a] and CARDILE *et al.* [2020], based on the results of several large-scale pullout tests [CARDILE *et al.*, 2014; CAZZUFFI *et al.*, 2014; MORACI *et al.*, 2014b; CARDILE *et al.*, 2016a], developed a theoretical method to determine the peak pullout resistance of extruded geogrids embedded in a compacted granular soil, taking into account the interference mechanism for closely spaced bearing members (*i.e.* for $S/B_{eq} < 50$). The method can be applied to soil-geogrid interfaces in which the scale effect is negligible. Moreover, it takes into account the non-linearity emerging in the failure envelope of compacted granular soils (due to the dilatancy effect), as well as the extensibility of reinforcements. The definition of such models is important both to improve the design and to optimise the industrial production of geosynthetics in terms of geometry, shape and stiffness, depending on the different applications for which they are designed. According to CARDILE *et al.* [2017a], the pullout resistance can be evaluated using the following equation:

$$P_R = 2 \cdot C_{\alpha S} \cdot \alpha_S \cdot L_R \cdot \sigma'_n \cdot tan\delta + C_{\alpha b} \cdot n_t \cdot n_{tb} \cdot A_b \cdot \sigma'_b \qquad (7)$$

where $C_{\alpha S}$ is a reduction coefficient to take into account the geogrid's area in which skin friction actually develops; δ is the mobilised friction angle between soil and the geogrid, which depends on soil dilatancy and reinforcement extensibility; $n_t = (L_R/S)$ is the number of geogrid's bearing members; n_{tb} is the number of nodes in a transverse element; A_b is the area of each rib element, which includes the single node and the bar portion between two nodes where the bearing resistance can be mobilised; and $C_{\alpha b}$ is a reduction coefficient taking into account the interference mechanism.

The first step of CARDILE *et al.* [2017a] research was to exclude from tests database those interfaces for which the scale effect was not negligible. To reach this goal, $\sigma'_b{}^{EXP}$ was calculated by equation (7) considering the peak pullout resistance obtained experimentally from tests carried out on the interfaces for which the interference effect was negligible ($S/B_{eq} > 50$), so as to set $C_{\alpha b} = 1$.

To be able to compare experimental $\sigma'_b{}^{EXP}$ values obtained for different soils, figure 11 shows the results normalized to the ($\sigma'_n \tan\varphi'$) value. From these results it is clear that the normalised bearing resistance starts to be independent from the average grain size for a ratio $B_{eq}/D_{50} > 10$, regardless of the normal effective stress. Once this threshold was found, all the tested interfaces with a ratio $B_{eq}/D_{50} > 10$ were analysed to determine the $C_{\alpha b}$ coefficient according to the following equation:

$$C_{\alpha b} = \frac{P_R^{Exp} - P_{RS}^{Theor}}{P_{RB}^{Theor}} = \frac{P_R^{Exp} - 2\alpha_S L_R \sigma'_n \tan\delta}{n_t \cdot n_{tb} \cdot A_b \cdot \sigma'_b} \quad (8)$$

where the peak pullout resistance P_R^{Exp} is obtained experimentally and σ'_b is evaluated by means of the equation proposed by MATSUI *et al.* [1996]. In order to take into account the reinforcement extensibility, which induces a progressive mobilisation of the interaction mechanisms, as well as the non-linear failure envelope of soil, P_{RS}^{Theor} component was evaluated using a shear strength angle that is the average value between the peak and the constant volume, while P_{RB}^{Theor} component was evaluated using the peak shear strength angles corresponding to the different normal effective stresses.

Figure 12 shows the interference reduction factors $C_{\alpha b}$, fitted by linear regression, for varying S/B_{eq} ratio. When $S/B_{eq} > 50$, the interference phenomenon can be considered negligible (meaning that the interference reduction factor $C_{\alpha b}$ is equal to one). Therefore, the interference reduction factor $C_{\alpha b}$ can be calculated as follows:

$$C_{\alpha b} \begin{cases} \alpha \cdot \dfrac{S}{B_{eq}} & \dfrac{S}{B_{eq}} \le 50 \\ 1 & \dfrac{S}{B_{eq}} > 50 \end{cases} \quad (9)$$

with constant coefficient α equal to 0.02. Summarising, the peak pullout resistance can be evaluated combining the equations (7) and (9).

Figure 13 shows one of the different comparisons between experimental and theoretical values of the peak pullout resistance evaluated for some selected interfaces investigated in the research [CARDILE *et al.*, 2017a], for varying normal effective stress. The results clearly prove the applicability of the proposed analytical method.

4.2.2. SOIL-GEOGRID BEHAVIOUR UNDER DIFFERENT TYPES OF LOAD

The mechanism whereby the pullout load is transferred along the extensible geosynthetic specimen embedded in a compacted soil could cause considerable reinforcement's elongation. Referring

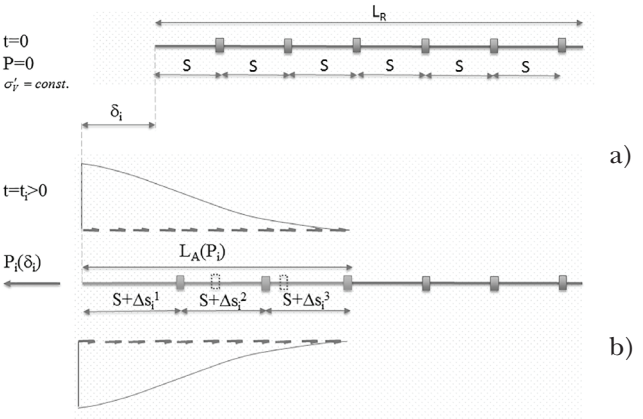

Fig. 14 – Pullout load transfer mechanism: a) P = 0; b) P > 0 [CARDILE *et al.*, 2016a].
Fig. 14 – Meccanismo di trasferimento del carico di sfilamento: a) P = 0; b) P > 0 [CARDILE et al., *2016a].*

to soil-geogrid interfaces (Fig. 14), when the pullout loading starts ($t_i > 0$ at the instant i), the geogrid's head moves of a quantity equal to δ_i and at the same time for the equilibrium only a small portion of the interface (L_A) mobilises equivalent shear stresses (function of skin friction and bearing resistance). At the same time tensile strains arise in the reinforcement, *i.e.* each portion between two transverse bars, S, withstands an elongation ΔS_i that becomes lesser for the portions more distant from the geogrid's head ($\Delta S_i^1 > \Delta S_i^2 > \Delta S_i^3$). Actually, the definition of distribution's shape and local magnitude of the mobilised shear stresses is very complex, depending on: loading and boundary conditions; physical properties and mechanical characteristics of soil; and structural, geometrical and mechanical characteristics of geosynthetic. The active length (L_A) is the portion of the geogrid specimen on which the mobilisation of the interaction mechanisms (skin friction and bearing resistance) withstands the applied load. Active length evaluation is important to understand the actual behaviour of soil-geosynthetic interfaces during the two phases of the pullout process, which are (i) load transfer phase and (ii) pullout phase.

Results obtained by pullout tests allow a better understanding of the pullout load transfer mechanism. Figure 15 shows the distribution of the transverse ribs' displacements along a geogrid specimen for different values of the applied pullout force, specifically for pullout tests carried out under monotonic loading conditions. The upper and lower graphs refer to long (L_R = 1.15 m) and short (L_R = 0.40 m) reinforcements, respectively. The tensile load transfer phase is plotted on the graphs to the left (Fig. 15a): the active length increases with increasing applied pullout force until this force reaches a limit value (triggering force, P_{ini}) that causes the movement of the last transverse rib (the dashed lines in

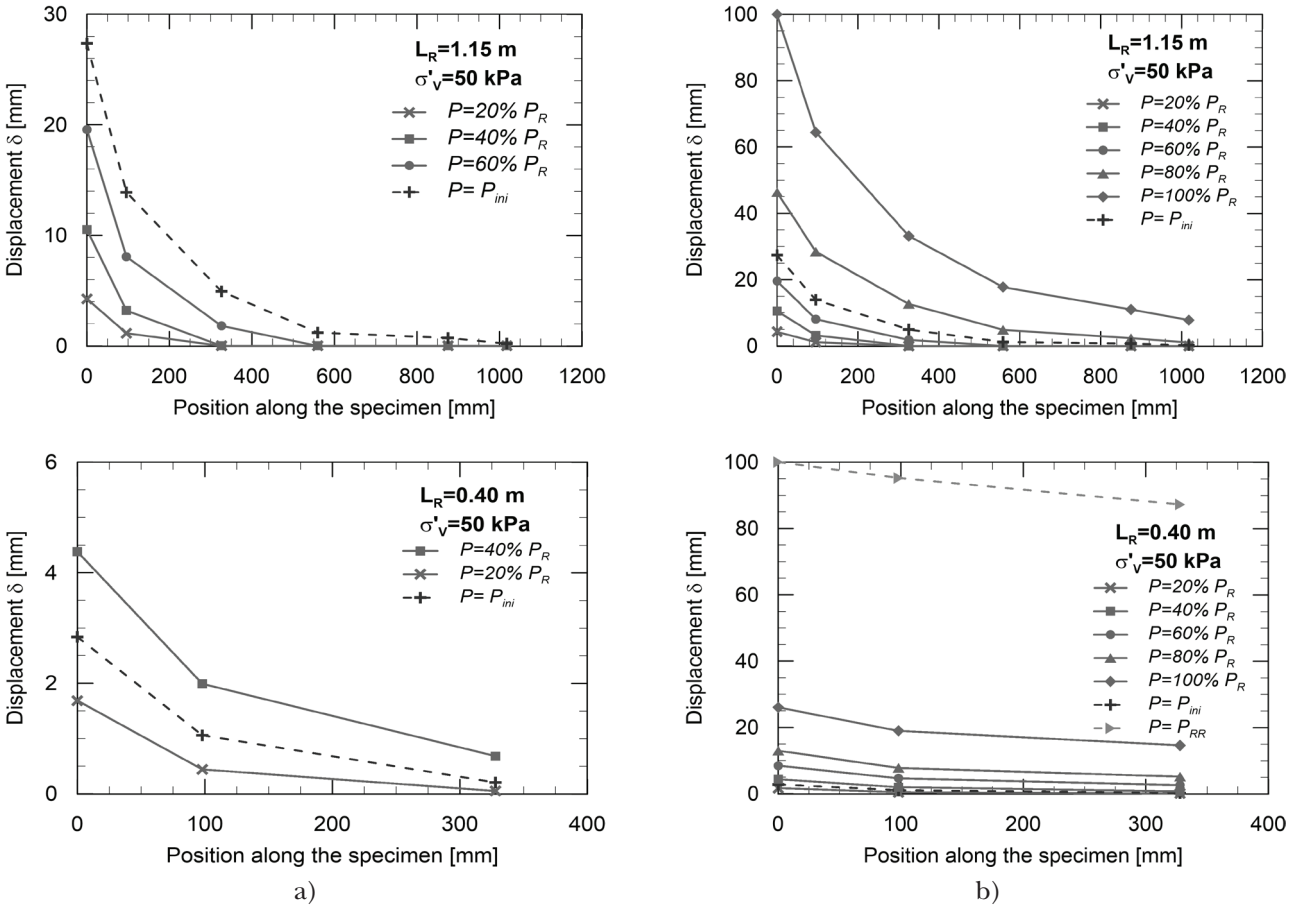

Fig. 15 – Distribution of the nodal displacements along the geogrid specimen for a fixed vertical effective stress (50 kPa) and for different values of the applied pullout force. The upper graphs refer to long reinforcements, while the lower graphs refer to short reinforcements, showing both a) the tensile load transfer phase and b) the pullout phase [CARDILE *et al.*, 2016a].
*Fig. 15 – Distribuzione degli spostamenti nodali lungo il provino di geogriglia per una data tensione verticale efficace (50 kPa) e per differenti valori della forza di sfilamento applicata. I grafici superiori si riferiscono a rinforzi lunghi, quelli inferiori a rinforzi corti, e mostrano a) la fase di trasferimento del carico e b) la fase di sfilamento [*CARDILE et al., *2016a].*

the graphs refer to these triggering forces). The pullout phase is plotted on the graphs to the right (Fig. 15b): it starts when the rear end of the geogrid begins to move, and in this case the active length coincides with the entire length of the specimen plus its elongation. The pullout phenomenon occurs when two adjacent curves (relative to different pullout loads) are parallel to each other, as it happened for the short reinforcement investigated in this research (bottom graph of Fig. 15b).

For extensible reinforcements, the non-linear distribution of shear stresses at the interface produces a non-linear distribution of transverse ribs' displacements. This non-linearity increases with decreasing reinforcement tensile stiffness. Vice versa, for rigid reinforcements (inextensible) the shear stress at the interface can be assumed to be constant along the specimen (in the case of specimens having a uniform surface). Considering geogrids with the same tensile stiffness, generally long reinforcement specimens show marked extensibility effects; this fact induces a progressive mobilisation of the interface interaction mechanisms that determine pullout resistance (upper graphs of Fig. 15). On the other hand, generally short reinforcement specimens show lower longitudinal strains (lower extensibility effects) and an almost immediate development of the interface interaction mechanisms along the specimen (lower graphs of Fig. 15).

In order to take into account that under pullout conditions load and elongation act on a reinforcement portion that varies during test's execution (*i.e.,* the active length), CARDILE *et al.* [2016a] defined the average longitudinal strain ε_A as the ratio of the recorded total elongation of the specimen, ΔL, to the difference between the related active length L_A and ΔL:

$$\varepsilon_A = \Delta L/(L_A - \Delta L) \tag{10}$$

As shown previously, the shear stress distribution along the reinforcement's length does not vary

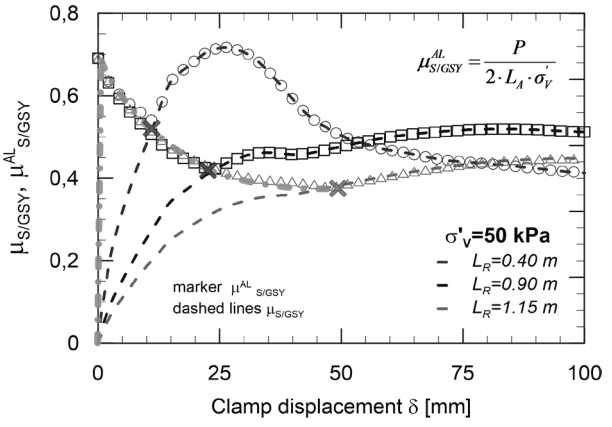

Fig. 16 – Pullout behaviour in terms of apparent coefficient of friction between soil and geosynthetic for a fixed vertical effective stress (50 kPa) and different specimen lengths [modified from CARDILE *et al.*, 2016a].
Fig. 16 – Comportamento a sfilamento in termini di coefficiente di attrito apparente mobilitato all'interfaccia terreno-geosintetico, per una data tensione verticale efficace (50 kPa) e differenti lunghezze del provino [modificato da CARDILE et al., *2016a].*

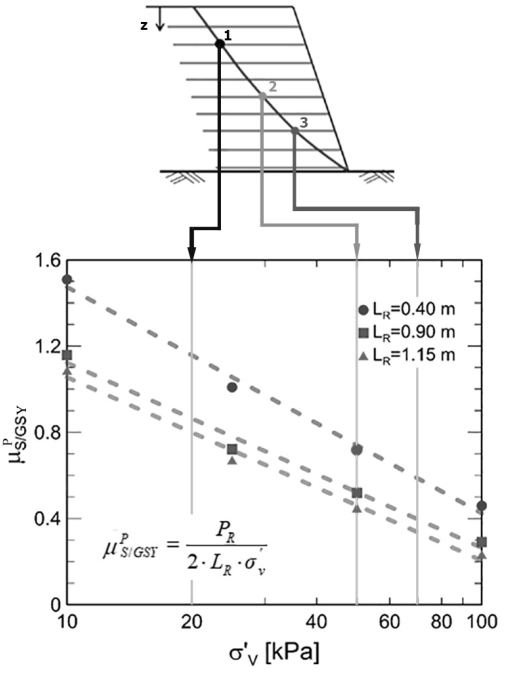

Fig. 17 – Peak apparent coefficient of friction for varying vertical effective stress, for different specimen lengths.
Fig. 17 – Coefficiente di attrito apparente di picco al variare della tensione verticale efficace, per differenti lunghezze del provino.

linearly [MORACI and RECALCATI, 2006; PERKINS and CUELHO, 1999; WANG *et al.*, 2014], but it can be replaced by an equivalent, uniform, average shear-stress distribution τ_{AL}. The ratio of the applied pullout load (P) to the double active length ($2\ L_A$) obtains the average shear stress:

$$\tau_{AL} = \frac{P}{2 \cdot L_A} \qquad (11)$$

The ratio between average shear stress value and vertical effective stress σ'_v is equal to the apparent coefficient of friction between soil and geosynthetic calculated using the active length, $\mu^{AL}_{S/GSY}$. Both the apparent coefficient of friction between soil and geosynthetic calculated using the total anchorage length ($\mu_{S/GSY}$, dashed lines) and the one obtained using the active length (lines made with symbols) are plotted in figure 16 for a fixed vertical effective stress and different lengths of specimens embedded in a compacted granular soil and subject to a monotonic load. During the load transfer phase, $\mu^{AL}_{S/GSY}$ values do not depend on the reinforcement length being they coincident (dash-dotted line), unlike those obtained using the total length. The large x-shaped markers instead show when the pullout phase starts. During the tensile load transfer phase, τ_{AL} decreases with increasing displacement of the first confined section δ (that is, clamp displacement), since the growing pullout force is mobilised on an active length that increases very rapidly during this phase. When the pullout phase starts, the active length becomes almost constant ($L_R+\Delta L$) while the pullout load continues to grow, consequently changing the trend in average shear stress that now increases with increasing displacement. In this phase, the interaction mechanisms are mobilised almost simultaneously along a short specimen (lowered extensibility effects) while in a long specimen they are mobilised progressively (more pronounced extensibility effects), thus producing a lower peak of the average shear stress that is mobilised at displacements higher than those concerning the peak of short reinforcements (progressive failure). Once longitudinal strain stops increasing, pullout occurs and average shear stress decreases rapidly.

The envelope of the results obtained in terms of peak conditions (Fig. 17) clearly shows the effects of the soil dilatancy at the interface: the peak apparent coefficient of friction between soil and geosynthetic decreases rapidly with increasing vertical effective stress acting on the interface.

Under cyclic tensile loads the pullout behaviour may be affected by frequency, amplitude and number of cycles of the cyclic loading history, as well as by the static tensile load level already acting on the geosynthetic when a cyclic load starts, in addition to the other abovementioned parameters.

As already stated previously, experimental researches performed only on reinforcing geosynthetics by using different cyclic loading histories allowed demonstrating that the material is not subjected to degradation (Fig. 8), thus maintaining

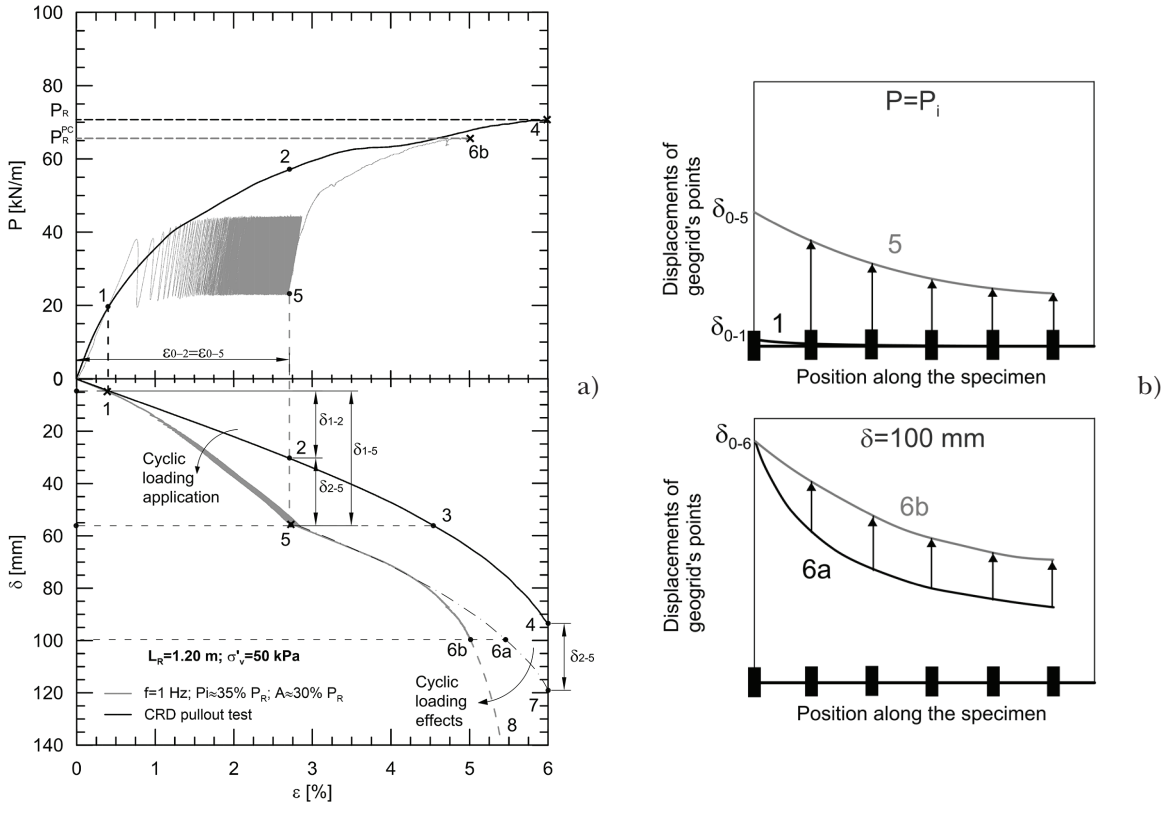

Fig. 18 – a) Comparison between P-ε and δ-ε trends obtained in CRD and multi-stage conditions, and b) qualitative distribution of the geogrid's points displacements in various phases of the test [CARDILE *et al.*, 2019].
*Fig. 18 – a) Confronto tra gli andamenti di P-ε e δ-ε ottenuti in condizioni monotone e multi-stage, e b) distribuzione qualitativa degli spostamenti dei punti della geogriglia in varie fasi della prova [*CARDILE et al., *2019].*

its short-term tensile strength. In order to verify whether or not the application of a cyclic load history could instead cause a decrease of the interface design parameters when the reinforcement is embedded in soil, different pullout tests were performed by CARDILE *et al.* [2019] and PISANO *et al.* [2019] using the same multi-stage (MS) test procedure described above for the wide-width MS tensile tests performed in-air. MS pullout tests were carried out by varying the applied vertical effective stress (10, 25, 50 and 100 kPa) and the cyclic load amplitude (equal to 30% and 45% of the peak pullout resistance P_R obtained by pullout tests under static conditions, carried out at the same confining pressure and constant rate of displacement (CRD) equal to 1mm per minute). The investigated frequency for 1000 cycles in total was equal to 1 Hz, while the starting tensile loading level P_i was chosen being equal to 35% P_R.

Figure 18a shows the MS and static results obtained for one of the analysed combinations (*i.e.* vertical effective stress equal to 50 kPa and cyclic load amplitude equal to 30% P_R), plotted in a double graph that correlates the displacement of the first confined section of the specimen, δ, with the confined average strain, ε, mobilised by a certain pullout load, *P*. The first outcome arising from the observation of points 1 and 5, which represent the beginning and the end of the cyclic phase respectively, is that the application of the cyclic load led to a higher geogrid's deformation (due to the viscous effects resulting from the application of a loading that can be considered constant on average over time) as well as to a higher displacement of the geogrid's head (the geogrid portion close to the clamp). This means that, at the end of the cyclic phase, the displacements of the internal points along the entire specimen length are greater than those mobilised in the reference static test at the same load level P_i are (top of Fig. 18b). Therefore, as the pullout process develops the pullout load is transferred on a geosynthetic's portion that increases rapidly during the cyclic phase, resulting in a reduction of the "reserve" of the pullout resistance available for the post-cyclic phase.

During the third phase, the interface tries again to mobilise the same pullout resistance that it would have mobilised if the cyclic stage had not occurred (showing a hardening behaviour), but this is not possible due to the degradation of the interface (while

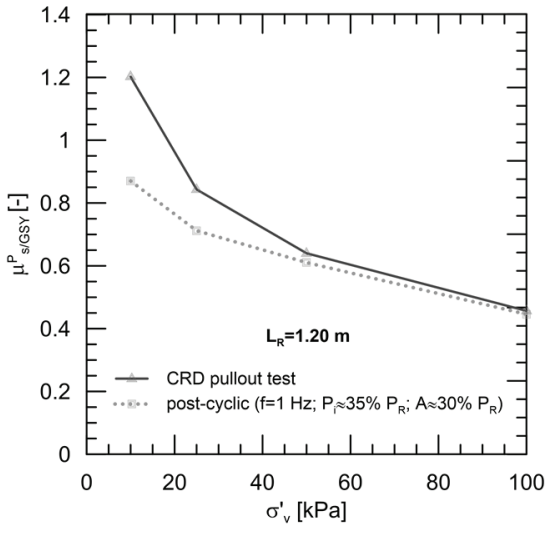

Fig. 19 – Comparison between peak apparent coefficients of friction evaluated under post-cyclic conditions and those obtained by means of CRD pullout tests for varying vertical effective stress [CARDILE *et al.*, 2019].
*Fig. 19 – Confronto tra il coefficiente di attrito apparente di picco valutato in condizioni post-cicliche e quello ottenuto da prove monotone, al variare della tensione verticale efficace [*CARDILE et al., *2019].*

the polymeric material does not degrade per se under the application of cyclic loading). Specifically, if the cyclic pullout load had not entailed a progression of the interaction mechanisms, the post-cyclic δ-ε curve would have followed the "ideal" trend of the monotonic curve (path 5-7). Actually, the curve bends more due to the effects of the cyclic load (path 5-8). This means that when the first confined section has reached the maximum displacement allowed by the pullout device (100 mm, bottom of Fig. 18b), the configuration of the displacements of the geogrid's internal points (6b) is different from the ideal trend's (6a): the geogrid starts to deform fewer while approaching the pullout limit state earlier. Therefore, this result can affect the mobilisation of the maximum pullout resistance, *i.e.* the peak apparent coefficient of friction between soil and geosynthetic. Reaching the pullout average strain corresponding to the peak pullout resistance P_R obtained under static conditions is theoretically still possible if the first confined section can do a further displacement. Nevertheless, this is possible as long as the pullout limit state has not been reached yet (that is when 5-8 curve reaches a vertical asymptote, Fig. 18a), since in that case the geogrid could no longer deform and consequently increase the mobilised pullout resistance.

For the specific test conditions, a decrease (up to about 30%) in the post-cyclic peak pullout resistance (*i.e.*, the peak apparent coefficient of friction) with respect to the values obtained in monotonic pullout tests has been observed (Fig. 19). Specifically with A being equal, this reduction increases with decreasing vertical effective stress (becoming negligible at the higher σ'_v values), while it increases with increasing cyclic load amplitude. The highlighted effects should be considered in the design of GRS structures in seismic areas appropriately reducing the interface parameters generally obtained by means of CRD pullout tests, since the reduction of the interface parameters involves the shallow reinforcement levels, which happen to be those more affected by the pullout limit state.

5. Some considerations on the advances in design practice

Several researches and case histories are available in literature, leading us in opening and facing some design questions that have not been fully solved yet. The answers to those questions, once clarified and recognised by the international standards, could lead to an optimisation of the design for GRS structures.

Measurements carried out on several full-scale instrumented GRS walls showed stresses and strains in the reinforcements (and, consequently, in the structures) that were a lot smaller than those modelled through the design parameters chosen in accordance with the provisions in codes, recommendations and standards. This implies that the design practice is very conservative; in the following paragraphs, the authors will attempt to answer some questions by debating about the design choices that usually lead to this.

5.1. Soil design parameters

The fact that the more used design approach is generally very conservative was evidenced by measurements made by several researchers, including WALTERS *et al.* [2002], BATHURST *et al.* [2005], and BATHURST [2014], on instrumented full-scale geosynthetic-reinforced soil structures.

These measurements allowed estimating empirically the effective horizontal stress, σ'_h, acting on the reinforced wall under different loading conditions. Such outcomes lead to the paradox of determining a coefficient of lateral earth pressure (K_h) lower than the active earth pressure coefficient (K_a) calculated using the shear strength angle chosen during the design phase:

$$K_h = \left[\frac{\sigma'_h(measured\ value)}{\sigma'_v}\right] < K_a\ (calculated\ value) \quad (12)$$

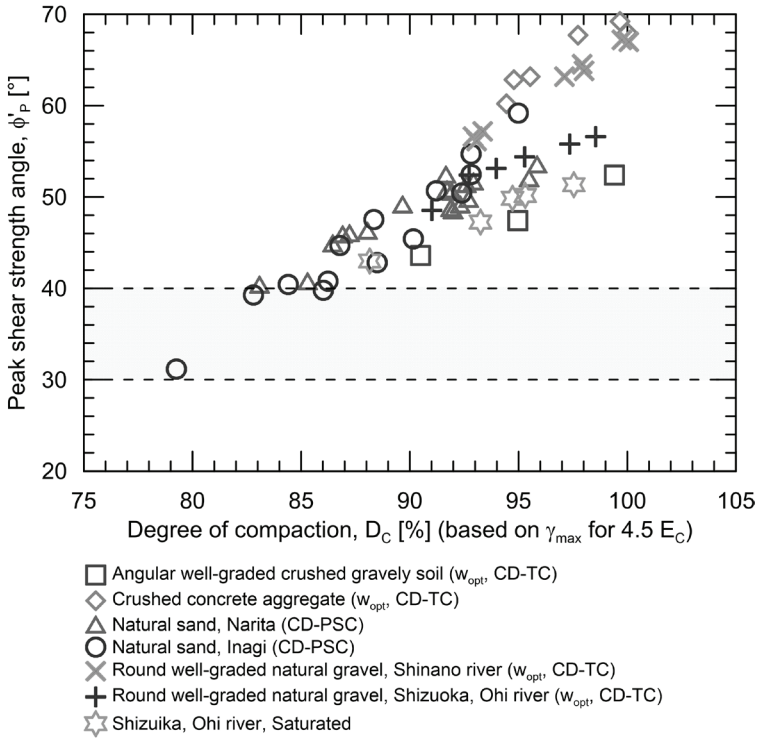

Fig. 20 – Peak shear strength angles for different degrees of compaction (at the optimum water content w_{opt} reached in laboratory compaction tests for a specified compaction energy E_c) obtained by triaxial (CD-TC) and plane strain (CD-PSC) compression tests (modified from HIRAKAWA *et al.*, 2008).

Fig. 20 – Angoli di resistenza al taglio di picco per differenti gradi di compattazione (al contenuto d'acqua optimum w_{opt} raggiunto in prove di costipamento di laboratorio per una data energia di compattazione E_c) ottenuti tramite prove triassiali consolidate drenate a temperatura controllata e prove di compressione in condizioni di deformazione piana (modificato da HIRAKAWA et al., *2008).*

The motivation for this result is attributable to several causes, many of which can be ascribed to the choice of the value for the shear strength angle of soil constituting the reinforced block. The reasons can be attributed to:

(i) *the effect of high compaction energy*;

The mechanical behaviour of a compacted soil is dilative, with a peak shear strength angle that is higher than the shear strength angle at constant volume: the magnitude of this gap increases with decreasing vertical effective stress.

Nowadays, the choice to use the shear strength angle mobilised at peak conditions is adopted formally by almost all the international recommendations regarding the design of reinforced soil structures; actually, they limit the choice within values that are more similar to shear strength angles at constant volume. In light of these considerations, it is possible to state that a reinforced structure having a well-compacted granular soil is designed often considering a soil shear strength far less than the strength the soil can actually mobilise, thus neglecting the effects due to the high level of compaction. Specifically, referring to a fill granular soil with up to 15% passing the No. 200 sieve, up to 60% passing the No. 40 sieve and plasticity index PI ≤ 6, the FHWA-NHI [2009] in agreement with AASHTO [2007] suggests using a shear strength angle equal to 34°; however, it is even possible to use larger values as long as they are not greater than 40°. In any case, such a choice must be documented with laboratory tests. Furthermore, cohesion must never be considered. The Japanese standard [PWRC, 2013] recommends the use of a peak shear strength angle equal to 35° for sands and 40° for gravels.

These aspects were highlighted by HIRAKAWA *et al.* [2008], who performed numerous plane strain (CD-PSC) and triaxial shear (CD-TC) tests varying the vertical effective stress from 20 to 50 kPa on different granular soils compacted at different degrees of compaction, which is defined as the ratio of the dry unit weight value in situ to the maximum dry unit weight obtained by laboratory compaction tests. The values obtained in terms of peak shear strength angle are considerably higher than those commonly used in design (Fig. 20). However, in the upper part of the GRS structure the effect of the "in-field" soil compaction caus-

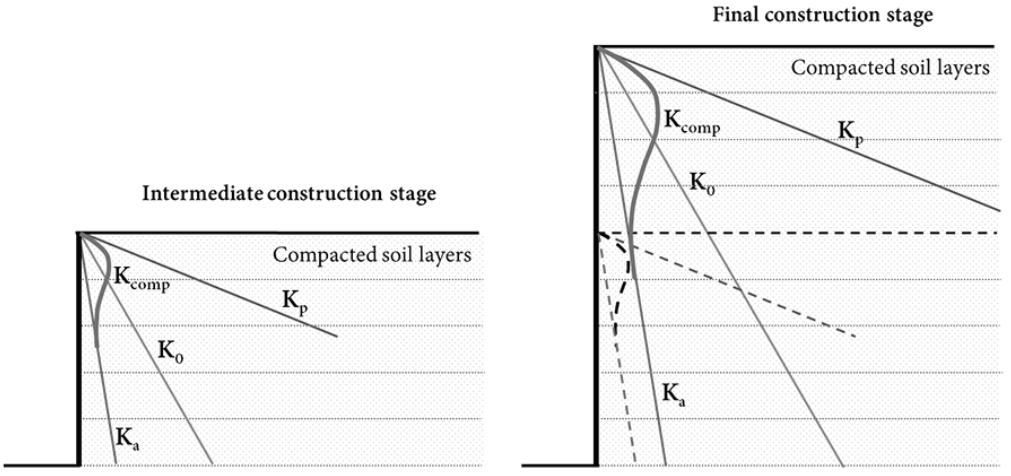

Fig. 21 – Qualitative trend of the horizontal stress acting on a reinforced earth retaining wall, due to lateral earth pressure and compaction (modified from MORACI, 2011).

Fig. 21 – Andamento qualitativo delle tensioni orizzontali agenti su un muro in terra rinforzata dovuto alla spinta laterale del terreno e alla compattazione (modificato da MORACI, 2011).

es a distribution of horizontal stresses, which are much higher (with a lateral earth pressure coefficient, K_{comp}, that can exceed the coefficient of lateral earth pressure at-rest, K_0, and even reach the passive earth pressure coefficient, K_p) than those used for calculating the tensile load acting on reinforcements by considering the active earth pressure coefficient, K_a. This aspect must be taken into account in the design (Fig. 21) and for this purpose, JEWELL [1996] relationship can be used:

$$0.45 \cdot (Q\gamma)^{1/2} \leq \sigma_{H_{COM}} \leq 0.9 \cdot (Q\gamma)^{1/2} \qquad (13)$$

where Q represents the weight of the roller compactor (kN/m).

(ii) *not considering the markedly curved strength envelope of dense granular soils*;
Soil mechanical behaviour is dilative in the range of the applied vertical effective stresses that characterise the typical heights of reinforced soil walls. In engineering practice, the actual curvilinear failure envelope of a compacted soil is usually replaced with a straight line characterised by specific intercept and slope values (soil cohesion and shear strength angle, respectively). This type of approximation can be satisfactory only for a certain range of values (the one for which the line has been obtained), unlike what happens outside of it (specifically at low confinement stresses). The alternative may be to define a peak shear strength angle that is secant and a function of the vertical effective stress. This fact implies that the shear strength angle to be used in the GRS structures design should be chosen so that varying with the depth where the geosynthetic is embedded.

(iii) *an inadequate geotechnical characterisation of the used soil;*
Unlike tests carried out in plane strain conditions, the most common and widespread triaxial and direct shear tests return results of the in-field actual condition that are cautious, especially at low confinement stresses.

(iv) *a possible contribution of suction*;
This effect acts in the soil constituting the reinforced block, producing an increase in the soil shear strength. Since this contribution could be erased in the case of saturation of the reinforced block, it is cautious to not consider it in geotechnical design.

(v) *a* further *contribution* which can be attributed to the effects *of the rigid facing system (if present) in combination with the toe-restraint effect* [HUANG *et al.*, 2010].
The mobilised resistance due to the toe-restraint effect can lead to a significant decrease of the soil thrust in the basal area of the retaining wall [LESHCHINSKY *et al.*, 2014; LESHCHINSKY and VAHEDIFARD, 2012]. This effect decreases significantly with increasing reinforced wall's height [MIRMORADI *et al.*, 2016]. This contribution is generally neglected in the design.

5.2. Geosynthetic and interface design parameters

Other motivations that involve a conservative design practice are related to the mechanical behav-

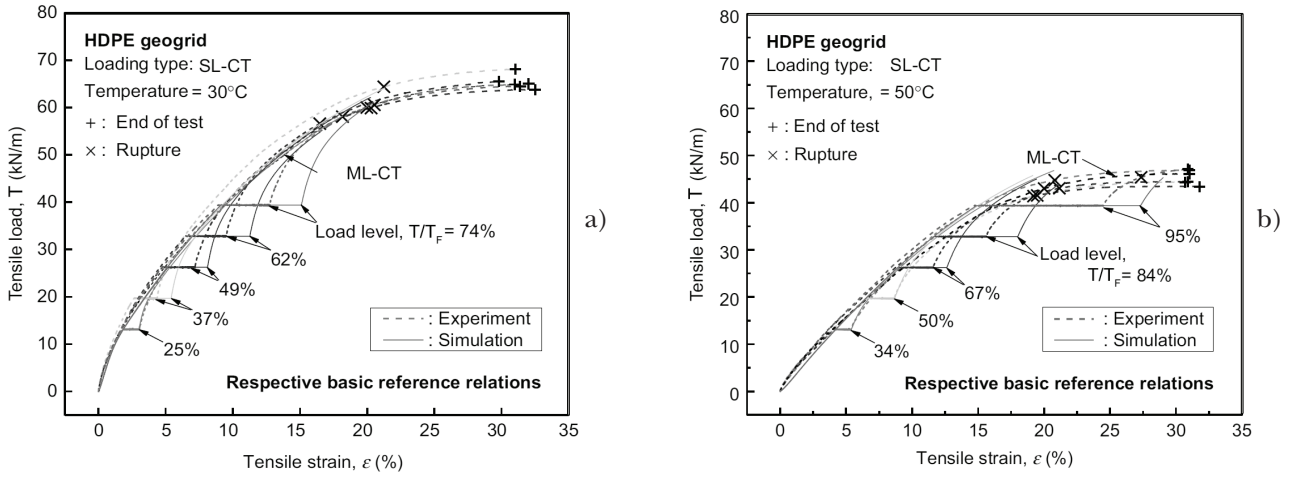

Fig. 22 – Comparison between monotonic and multi-stage (with creep phase) test results carried out on HDPE geogrid at different temperatures: a) T = 30°C; b) T = 50°C [modified from CHANTACHOT *et al.*, 2018].

Fig. 22 – Confronto tra i risultati di prove monotone e multi-stage (con fase a carico costante) condotte su geogriglie in HDPE a differenti temperature: a) T = 30°C; b) T = 50°C [modificato da CHANTACHOT et al.*, 2018].*

iour of geosynthetics, namely to the tensile strength that can be made available by the chosen reinforcement. In fact, the design tensile strength is considerably higher than the one mobilised on reinforcement under serviceability conditions (even considering, in seismic design, the potential aliquot mobilised under a seismic event). This is mostly due to the fact that the creep reduction factor is determined considering a tensile load which causes the creep rupture at the design life, thus assuming that this load is kept constant all the time. Actually, the tensile load acting on reinforcements in ordinary *(i.e.* non-critical) conditions is considerably lower than the sustained load used to obtain creep design reduction factors.

Moreover, under seismic load combinations, using the creep reduction factor on the seismic aliquot could be further conservative. For this reason, the Japanese Railway Design Code specifies that the seismic load combinations must not take into account the creep reduction factor to calculate the long-term tensile strength, unlike the static loading combinations. Even the French code [NF P 94-270, 2009] states that the long-term tensile strength must be calculated without considering the reduction factor due to creep when designing in seismic conditions. One of the reasons for this choice is that the creep phenomenon is generally considered to start after the conclusion of the geosynthetic's biochemical degradation process, while in reality the two processes begin simultaneously [KONGKITKUL *et al.*, 2007] and this could lead to a combined reduction factor which is lower than those currently used. Another reason is that, according to HIRAKAWA *et al.* [2003], KONGKITKUL *et al.* [2004], TATSUOKA [2008] and CHANTACHOT *et al.* [2018], the creep effects do not induce a material degradation in contrast to chemical, physical, mechanical, environmental and biological agents that can produce a degradation of the material's structure. The experimental results showed that the tensile strength obtained by monotonic tensile tests at constant temperature (ML-CT) is equivalent to the one obtained in tensile tests having a stage that applies a long-term static load (sustained load, SL-CT, *e.g.* for 30 days) before reaching the peak (Fig. 22), regardless the temperature or load level (which is the level in which the sustained load is applied, chosen as a percentage of the maximum tensile load T_F obtained by short-term monotonic tensile tests). Therefore, since creep is not a degradation phenomenon but exclusively a viscous response [KONGKITKUL *et al.*, 2007; TATSUOKA *et al.*, 2004], when the reinforcement is suddenly subjected to a seismic input (that can be considered a constant load on average over time), it still can mobilise the ultimate tensile strength T_F.

Another important consideration to point out is that international codes, recommendations and standards use creep reduction factors obtained by results of tensile tests carried out without soil confinement, while the presence of a compacted soil could lead to different results.

FRANCA and BUENO [2011] developed a prototype test apparatus to analyse geosynthetic tensile creep behaviour in soil-confined conditions by performing temperature-controlled tests. Despite the test limits due to scale effects and the limited sustaining of the tensile load (only 100 hours), this research shows the development of strains under constant tensile load that are smaller than those obtained from corresponding creep tests performed without soil confinement (Fig. 23).

To better understand the tensile creep effects due to a sustained pullout load (constant over

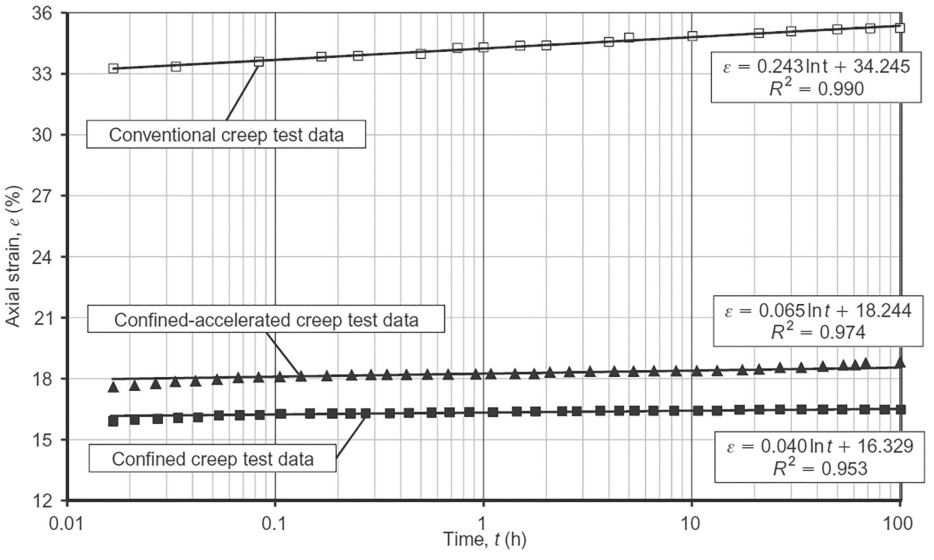

Fig. 23 – Creep test results [FRANCA and BUENO, 2011].
Fig. 23 – Risultati di prove di creep [FRANCA and BUENO, 2011].

time), recently CARDILE *et al.* [2021] designed and built a large-scale prototype pullout apparatus. The equipment allows the application of a constant pullout load through a completely mechanical gear wheel system. The vertical load application system is pneumatic, while the displacements of the geogrid's internal points are measured by means of displacement transducers connected to the different geogrid transverse bars. The clamp system is internal in order to guarantee a constant anchorage length for the entire duration of the test, allowing investigation of the possible tensile rupture due to confined tensile creep. The first creep confined pullout tests are currently in progress on two twin apparatus, on two identical specimens of the same extruded HDPE geogrid embedded in a compacted well-graded sand with gravel. The effects due to sustaining two different pullout load levels over time (equal to 50% and 70% of the peak pullout resistance obtained by a pullout test performed at constant rate of displacement equal to 1 mm per minute and at the same vertical effective stress) have been analysed.

Strains measured in the geogrid's portion closer to the clamp after 20 hours show a lower growth gradient compared to those obtained by in-air tensile tests. If this trend continues (10000 hours have been investigated until now), the time necessary to reach the creep rupture in pullout conditions would be longer than that obtained by conventional in-air tensile tests, with a consequent reduction of the creep reduction factor extrapolated (from accelerated laboratory tests) to the design life.

Finally, another assumption that leads to a conservative design is to take into account the lower value of the interface parameter $\mu^P_{S/GSY}$, while the correct way to proceed would be to adopt different $\mu^P_{S/GSY}$ values for each reinforcement level, varying with the depth where any of them is embedded.

6. Critical aspects of the construction practice

After half a century's experience, it is now simpler to identify the critical aspects concerning the construction practice for GRS structures. A recent study carried out by KOERNER and KOERNER [2013] provided interesting statistics related to the damage occurred on 171 geosynthetic-reinforced soil walls located mainly in North America. This research allows extrapolating useful design recommendations. In most of the examined case histories, the damage's causes could be traced back to a faulty construction of the structure related to a lack of proper supervision by construction manager/work supervisor, to inappropriate choices made to optimise company revenues, and to a lacking of training of the involved construction workers. It seems almost superfluous to point out that a strict control during construction is much less expensive than resolving the damage caused thereafter. Damages occurred mainly within a few years of the construction (86% within 4 years, 67% within 2 years) and the causes were almost exclusively (98%) attributable to: (i) poor soil compaction (72%); (ii) use of silty or clayey soils for the construction of the reinforced block, characterised by low hydraulic conductivity but already available on site, thus saving on the use of more expensive quarry material (61%); (iii) the presence of internal or external water in the reinforced block, with consequent mobilisation of hydraulic thrust forces not generally considered in

the design (60% - lack or inadequacy of the internal and external drainage system, water pipes within the soil reinforced block, etc.). For these reasons internal and external drainage systems, as well as the waterproofing of the top surfaces of the reinforced structure, must be carefully designed based on the needs of the specific case, and described in the working drawings in detail.

7. Conclusions

Nowadays, the use of geosynthetics provides a mature technological solution that helps designers to solve geotechnical and environmental problems focusing on development and protection of territory. Geosynthetics permit to reduce the environmental impact of traditional geotechnical and environmental engineering structures, improving their sustainability and increasing the resilience of the Planet.

The paper analysed the advancement in the design practice of geosynthetic reinforced soil structures, going through short- and long-term laboratory test results on both reinforcements and soil-geosynthetic interfaces, as well as the modelling of the interaction under pullout conditions ruling one of the mechanisms of the internal stability.

Moreover, the reasons for which the design choices lead to a very conservative design practice were discussed. Regarding the filling soil in the reinforced block, the reasons are connected to using a shear strength angle evaluated without considering the effects of the soil dilatancy and the effects of a soil compaction high level adopted during the construction phase. In relation to the design mechanical parameters of the reinforcement, the long-term tensile strength values actually adopted are generally conservative because standards in force do not take into account neither the positive effect of the soil confinement on geosynthetic's tensile creep, nor the fact that this phenomenon does not cause a degradation of the polymeric materials (thus having the possibility to omit it in the potential seismic aliquot). On the other hand, the actual design practice defines an interface parameter which does not consider the possible degradation of the interface due to cyclic or seismic loads. As remarked by the authors in the paper, this effect, highlighted in a recent experimental research, should be considered in the design of GRS structures in seismic areas.

Finally, the critical aspects concerning the construction practice were highlighted, gathering that it is necessary to improve the education of students, professionals and constructor companies, still often too far from knowing and using geosynthetics, which continue to be defined as innovative almost half a century after their first applications.

References

ABDI M.R., ARJOMAND M.A. (2011) – *Pullout tests conducted on clay reinforced with geogrid encapsulated in thin layers of sand*. Geotextiles and Geomembranes, 29, pp.588-595.

AYDOGMUS T., ALEXIEW D., KLAPPERICH H. (2007) – *Laboratory testing of interaction performance of PVA geogrids embedded in stabilized cohesive soils*. 14th European Conference on Soil Mechanics and Geotechnical Engineering, Madrid, Spain, pp. 1417-1420.

AASHTO (2007) – *LRFD Bridge Design Specifications*. 4th Edition, 2007, with 2008 and 2009 Interim Revisions, American Association of State Highway and Transportation Officials (AASHTO), Washington, DC, USA.

AASHTO T 99 (2015) – *Standard Method of Test for Moisture-Density Relations of Soils Using a 2.5-kg (5.5-lb) Rammer and a 305-mm (12-in.) Drop*. American Association of State Highway and Transportation Officials (AASHTO), Washington, DC, USA.

AASHTO T 180 (2015) – *Standard Method of Test for Moisture-Density Relations of Soils Using a 4.54-kg (10-lb) Rammer and a 457-mm (18-in.) Drop*. American Association of State Highway and Transportation Officials (AASHTO), Washington, DC, USA.

AASHTO T 289 (1991) – *Standard Method of Test for Determining pH of Soil for Use in Corrosion Testing*. American Association of State Highway and Transportation Officials (AASHTO), Washington, DC, USA.

AASHTO T 290-95 (2016) – *Standard Method of Test for Determining Water-Soluble Sulfate Ion Content in Soil*. American Association of State Highway and Transportation Officials (AASHTO), Washington, DC, USA.

ASTM D698 (2012) – *Standard Test Methods for Laboratory Compaction Characteristics of Soil Using Standard Effort (12 400 ft-lbf/ft3 (600 kN-m/m3))*. American Society for Testing and Materials (ASTM), West Conshohocken, PA, USA.

ASTM D1556 (2015) – *Standard Test Method for Density and Unit Weight of Soil in Place by Sand-Cone Method*. American Society for Testing and Materials (ASTM), West Conshohocken, PA, USA.

ASTM D1557 (2012) – *Standard Test Methods for Laboratory Compaction Characteristics of Soil Using Modified Effort (56,000 ft-lbf/ft3 (2,700 kN-m/m3))*. American Society for Testing and Materials (ASTM), West Conshohocken, PA, USA.

ASTM D2167 (2015) – *Standard Test Method for Density and Unit Weight of Soil in Place by the Rubber Balloon Method*. American Society for Testing and Materials (ASTM), West Conshohocken, PA, USA.

ASTM D2488 (2017) – *Standard Practice for Description and Identification of Soils (Visual-Manual Procedures)*. American Society for Testing and Materials (ASTM), West Conshohocken, PA, USA.

ASTM D4327 (2017) – *Standard Test Method for Anions in Water by Suppressed Ion Chromatography*. American Society for Testing and Materials (ASTM), West Conshohocken, PA, USA.

ASTM D4972 (2019) – *Standard Test Method for pH of soils*. American Society for Testing and Materials (ASTM), West Conshohocken, PA, USA.

ASTM D5321 (2019) – *Standard Test Method for Determining the Shear Strength of Soil-Geosynthetic and Geosynthetic-Geosynthetic Interfaces by Direct Shear*. American Society for Testing and Materials (ASTM), West Conshohocken, PA, USA.

ASTM D6637 (2015) – *Standard Test Method for Determining Tensile Properties of Geogrids by the Single or Multi-Rib Tensile Method*. American Society for Testing and Materials (ASTM), West Conshohocken, PA, USA.

ASTM D6706-01 (2013) – *Standard Test Method for Measuring Geosynthetic Pullout Resistance in Soil*. American Society for Testing and Materials (ASTM), West Conshohocken, PA, USA.

ASTM D6938 (2017) – *Test Method for in-place Density and Water Content of Soil and Soil-Aggregate by Nuclear Methods (Shallow Depth)*. American Society for Testing and Materials (ASTM), West Conshohocken, PA, USA.

ASTM D 7737M (2015) – *Standard Test Method for Individual Geogrid Junction Strength*. American Society for Testing and Materials (ASTM), West Conshohocken, PA, USA.

BATHURST R.J. (2014) – *Challenges and recent progress in the analysis, design and modelling of geosynthetic reinforced soil walls*. 10th International Conference on Geosynthetics, ICG 2014, Berlin, Germany, pp. 180-218.

BATHURST R.J., ALLEN T.M., WALTERS D. (2005) – *Reinforcement loads in geosynthetic walls and the case for a new working stress design method*. Geotextiles and Geomembranes, 23, pp. 287-322.

BATHURST R.J., CAI Z. (1994) – *In-Isolation cyclic load-extension behavior of two geogrids*. Geosynthetics International, 1, pp. 1-19.

BERGADO D.T., CHAI J.C. (1994) – *Pullout force/displacement relationship of extensible grid reinforcements*. Geotextiles and Geomembranes, 13, pp. 295-316.

BERGADO D.T., SHIVASHANKAR R., ALFARO M.C., CHAI J.-C., BALASUBRAMANIAM A.S. (1993) – *Interaction behaviour of steel grid reinforcements in a clayey sand*. Géotechnique, 43, pp. 589-603.

BHAT G., KANDAGOR V. (2014) – *Synthetic polymer fibers and their processing requirements*. In: Zhang D., (Ed.), "Advances in Filament Yarn Spinning of Textiles and Polymers". Woodhead Publishing, pp. 3-30.

BOURDEAU P.L. (1989) – *Modeling of membrane action in a two-layer reinforced soil system*. Computers and Geotechnics, 7, pp. 19-36.

BOURDEAU P.L., HARR M.E., HOLTZ R.D. (1982) – *Soil-fabric interaction: an analytical model*. 2nd International Conference on Geotextiles, Las Vegas (USA), pp. 387-391.

BRANDL H. (2011) – *Geosynthetics applications for the mitigation of natural disasters and for environmental protection*. Geosynthetics International, 18, pp. 340-390.

BS 8006 (2010) – *Code of practice for strengthened/reinforced soils and other fills*. British Standards Institution, London, UK, 249 p.

BS EN 771-3 (2011) – *Specification for masonry units. Aggregate concrete masonry units (dense and lightweight aggregates)*. European Committee for Standardization, Brussels.

BS EN 12878 (2014) – *Pigments for the colouring of building materials based on cement and/or lime*. Specifications and methods of test. European Committee for Standardization, Brussels.

BS EN ISO 12957-1 (2018) – *Geosynthetics. Determination of friction characteristics. Direct shear test*. European Committee for Standardization in collaboration with the International Standardization Organization, Brussels.

CALVARANO L.S., GIOFFRÈ D., CARDILE G., MORACI N. (2014) – *A stress transfer model to predict the pullout resistance of extruded geogrids embedded in compacted granular soils*. 10th International Conference on Geosynthetics, ICG 2014, Berlin, Germany, pp. 1153-1160.

CARDILE G., CALVARANO L.S., GIOFFRÈ D., MORACI N. (2014) – *Experimental evaluation of the pullout active length of different geogrids*. 10th International Conference on Geosynthetics, ICG 2014, Berlin, Germany, pp. 1184-1190.

CARDILE G., GIOFFRÈ D., MORACI N., CALVARANO L.S. (2017a) – *Modelling interference between the geogrid bearing members under pullout loading conditions*. Geotextiles and Geomembranes, 45, pp. 169-177.

CARDILE G., MORACI N., CALVARANO L.S. (2016a) – *Geogrid pullout behaviour according to the experimental evaluation of the active length*. Geosynthetics International, 23, pp. 194-205.

CARDILE G., MORACI N., PISANO M. (2016b) – *In-air Tensile Load-strain Behaviour of HDPE Geogrids Under Cyclic Loading*. Procedia Engineering, 158, pp. 266-271.

CARDILE G., MORACI N., PISANO M. (2017b) – *Tensile behaviour of an HDPE geogrid under cyclic loading: experimental results and empirical modelling*. Geosynthetics International, 24, n. 1, pp. 95-112.

CARDILE G., PISANO M., MORACI N. (2019) – *The influence of a cyclic loading history on soil-geogrid interaction under pullout condition*. Geotextiles and Geomembranes, 47, n. 4, pp. 552-565.

CARDILE G., PISANO M., MORACI N. (2020) – *A Predictive Model for Pullout Bearing Resistance of Geogrids Embedded in a Granular Soil*. In: F. Calvetti, F. Cotecchia, A. Galli, C. Jommi (Eds.), Geotechnical Research for Land Protection and Development.

Springer International Publishing, Cham, Lecture Notes in Civil Engineering, 40, pp. 438-445.

CARDILE G., PISANO M., RECALCATI P., MORACI N. (2021) – *Una nuova apparecchiatura di sfilamento per lo studio del comportamento a lungo termine di interfacce terreno-geosintetico*. Convegno Nazionale di Geotecnica, 7-9 luglio 2021, Reggio Calabria, 8 p.

CAZZUFFI D., CALVARANO L.S., CARDILE G., MORACI N., RECALCATI P. (2011) – *European experience in pullout tests: The influence of geogrid's geometry and structure on interface behaviour*. Geosynthetics, 29, pp. 42-51.

CAZZUFFI D., MORACI N., CALVARANO L.S., CARDILE G., GIOFFRÈ D., RECALCATI P. (2014) – *The influence of vertical effective stress and of geogrid length on interface behaviour under pullout conditions*. Geosynthetics, 32, pp. 40-50.

CHANG D.T.-T., CHANG F.C., YANG G.S., YAN C.Y. (2000) – *The influence factors study for geogrid pullout test*. ASTM STP1379-EB Grips, Clamps, Clamping Techniques, and Strain Measurement for Testing of Geosynthetics, 14 p.

CHANTACHOT T., KONGKITKUL W., TATSUOKA F. (2018) – *Effects of temperature rise on load-strain-time behaviour of geogrids and simulations*. Geosynthetics International, 25, pp. 287-303.

COOKE T.F., REBENFELD L. (1988) – *Effect of chemical composition and physical structure of geotextiles on their durability*. Geotextiles and Geomembranes, 7, pp. 7-22.

CORREIA N.S., ZORNBERG J.G. (2016) – *Mechanical response of flexible pavements enhanced with geogrid-reinforced asphalt overlays*. Geosynthetics International, 23, pp. 183-193.

DIXON N. (2010) – *Soil-geosynthetic interaction: interface behaviour*. 9th International Conference on Geosynthetics. International Geosynthetics Society, Guaruja, Brazil, pp. 563-582.

DYER M.R. (1985) – *Observations of the stress distribution in crushed glass with applications to soil reinforcement*. Magdalene College, University of Oxford, Michaelmas Term, 220 p.

EBGEO (2010) – *Recommendations for design and analysis of earth structures using geosynthetic reinforcements*. German Geotechnical Society (Deutsche Gesellschaft für Geotechnik e. V., DGGT).

FANG Y.S., YANG Y.C., CHEN T.J. (2003) – *Retaining walls damaged in the Chi-Chi earthquake*. Canadian Geotechnical Journal, 40, pp. 1142-1153.

FARRAG K., MORVANT M. (2000) – *Effect of clamping mechanism on pullout and confined extension tests*. ASTM STP1379-EB Grips, Clamps, Clamping Techniques, and Strain Measurement for Testing of Geosynthetics, pp. 89-96.

FHWA-NHI (2009) *Design and Construction of Mechanically Stabilized Earth Walls and Reinforced Soil Slopes*. National Highway Institute Federal Highway Administration U.S. Department of Transportation, Washington, D.C., vol. I, 332 p. (FHWA-NHI-10-024) and vol. II, 404 p. (FHWA-NHI-10-025).

FRANCA F.A.N., BUENO B.S. (2011) – *Creep behavior of geosynthetics using confined accelerated tests*. Geosynthetics International, 18, n. 5, pp. 242-254.

GIROUD J.P., NOIRAY L. (1981) – *Geotextile-reinforced unpaved road design*. Journal of Geotechnical Engineering, 107, pp. 1233-1254.

HAYASHI S., ALFARO M.C., WATANABE K. (1996) – *Dilatancy effects of granular soil on the pullout resistance of strip reinforcement*. International Symposium on Earth Reinforcement, Fukuoka, Kyushu, Japan, pp. 39-44.

HIRAKAWA D., KAWAHARAZONO M., TATSUOKA F. (2008) – *Effect of compaction conditions on strength and deformation characteristics of backfill materials*. Journal of Japanese Society for Civil Engineers, 64, pp. 253-266.

HIRAKAWA D., KONGKITKUL W., TATSUOKA F., UCHIMURA T. (2003) – *Time-dependent stress–strain behaviour due to viscous properties of geogrid reinforcement*. Geosynthetics International, 10, pp. 176-199.

HUANG B., BATHURST R.J., HATAMI K., ALLEN T.M. (2010) – *Influence of toe restraint on reinforced soil segmental walls*. Canadian Geotechnical Journal, 47, pp. 885-904.

HUANG C.-C., WANG W.-C. (2005) – *Seismic displacement of a geosynthetic-reinforced wall in the 1995 Hyogo-ken Nambu earthquake*. Soils and Foundations, 45, pp. 1-10.

HUANG C.C. (2000) – *Investigations of soil retaining structures damaged during the chi-chi (Taiwan) earthquake*. Journal of the Chinese Institute of Engineers, 23, pp. 417-428.

ISO 554 (1976) – *Standard atmospheres for conditioning and/or testing – Specifications*. International Organization for Standardization, ISO, Ginevra.

ISO/TR 20432 (2007) – *Guidelines to the determination of long-term strength of geosynthetics for soil reinforcement*. International Organization for Standardization, ISO, Ginevra.

ISO/TS 13434 (2008) – *Geosynthetics — Guidelines for the assessment of durability*. International Organization for Standardization, ISO, Ginevra.

JACOBS F., ZIEGLED M., VOLLMERT L., EHRENBERG H. (2014) – *Explicit design of geogrids with a nonlinear interface model*. 10th International Conference on Geosynthetics, ICG 2014, Berlin, Germany, pp. 609-616.

JEWELL R.A. (1990) – *Reinforcement bond capacity*. Géotechnique, 40, pp. 513-518.

JEWELL R.A. (1996) – *Soil Reinforcement with geotextile*. CIRIA Thomas Telford, London.

JEWELL R.A., MILLIGAN G.W.E., SARSBY R.W., DUBOIS D. (1985) – *Interaction between soil and geogrids*. In: T. Telford, (Ed.), "Symposium on Polymer Grid Reinforcement in Civil Engineering", pp. 18-30.

JOHNSTON R.S., ROMSTAD K.M. (1989) – *Dilation and*

boundary effects in large scale pullout test. 12th International Conference on Soil Mechanics and Foundation Engineering, Rio De Janeiro, 2, pp. 1263-1266.

KANG Y., NAM B., ZORNBERG J.G., CHO Y.-H. (2015) – *Pullout resistance of geogrid reinforcement with in-plane drainage capacity in cohesive soil.* KSCE Journal of Civil Engineering, 19, pp. 602-610.

KOERNER R.M., KOERNER G.R. (2013) – *A database, statistics and recommendations regarding 171 failed geosynthetic reinforced mechanically stabilized earth (MSE) walls.* Geotextiles and Geomembranes, 40, pp. 20-27.

KOFFLER A., CHOURA M., BENDRISS A., ZENGERINK E. (2008) – *Geosynthetics in protection against erosion for river and coastal banks and marine and hydraulic construction.* Journal of Coastal Conservation, 12, pp. 11-17.

KONGKITKUL W., HIRAKAWA D., TATSUOKA F., UCHIMURA T. (2004) – *Viscous deformation of geosynthetic reinforcement under cyclic loading conditions and its model simulation.* Geosynthetics International, 11, pp. 73-99.

KONGKITKUL W., TABSOMBUT W., JATURAPITAKKUL C., TATSUOKA F. (2012) – *Effects of temperature on the rupture strength and elastic stiffness of geogrids.* Geosynthetics International, 19, pp. 106-123.

KONGKITKUL W., TATSUOKA F., HIRAKAWA D. (2007) – *Creep rupture curve for simultaneous creep deformation and degradation of geosynthetic reinforcement.* Geosynthetics International, 14, pp. 189-200.

KOSEKI J., BATHURST R.J., GULER E., KUWANO J., MAUGERI M. (2006) – *Seismic stability of reinforced soil walls.* 8th International Conference on Geosynthetics, Yokohama, Japan, 1, 51-77.

KOSEKI J., HAYANO K., WATANABE K., HUANG C.C. (2000) – *Damage to retaining walls caused by the 1999 Chi-Chi earthquake and model tests on seismic behaviour of retaining walls.* International Workshop on Annual Commemoration of Chi-Chi earthquake, Taipei, pp. 251-262.

KUWANO J., MIYATA Y., KOSEKI J. (2014) – *Performance of reinforced soil walls during the 2011 Tohoku earthquake.* Geosynthetics International, 21, pp. 179–196.

KWON J., TUTUMLUER E., KIM M. (2005) – *Development of a mechanistic model for geosynthetic-reinforced flexible pavements.* Geosynthetics International, 12, pp. 310-320.

LESHCHINSKY D., KANG B., HAN J., LING H. (2014) – *Framework for Limit State Design of geosynthetic-reinforced walls and slopes.* Transportation Infrastructure Geotechnology, 1, pp. 129-164.

LESHCHINSKY D., VAHEDIFARD F. (2012) – *Impact of toe resistance in reinforced masonry block walls: design dilemma.* Journal of Geotechnical and Geoenvironmental Engineering, 138, pp. 236-240.

LING H., LESHCHINSKY D. (2005) – *Failure analysis of modular-block reinforced-soil walls during earthquakes.* Journal of Performance of Constructed Facilities, 19, pp. 117-123.

LING H.I., LESHCHINSKY D., CHOU N.N.S. (2001) – *Post-earthquake investigation on several geosynthetic-reinforced soil retaining walls and slopes during the Ji-Ji earthquake of Taiwan.* Soil dynamics and earthquake engineering, 21, pp. 297-313.

LIU H., LING H.I. (2006) – *Modeling cyclic behavior of geosynthetics using mathematical functions combined with Masing rule and bounding surface plasticity.* Geosynthetics International, 13, pp. 234-245.

LIU H., LING H.I. (2007) – *Unified elastoplastic-viscoplastic bounding surface model of geosynthetics and its applications to geosynthetic reinforced soil-retaining wall analysis.* Journal of Engineering Mechanics, 133, pp. 801-815.

LOPES M.L., LADEIRA M. (1996) – *Influence of confinement, soil density and displacement rate on soil-geogrid interaction.* Geotextiles and Geomembranes, 14, pp. 543-554.

LOVE J.P., BURD H.J., MILLIGAN G.W.E., HOULSBY G.T. (1987) – *Analytical and model studies of reinforcement of a layer of granular fill on a soft clay subgrade.* Canadian Geotechnical Journal, 24, pp. 611-622.

MADHAV M.R., POOROOSHASB H.B. (1988) – *A new model for geosynthetic reinforced soil.* Computers and Geotechnics, 6, pp. 277-290.

MASINI L., CALLISTO L., RAMPELLO S. (2015) – *An interpretation of the seismic behaviour of reinforced-earth retaining structures.* Géotechnique, 65, pp. 349-358.

MATSUI T., SAN K.C., NABESHIMA Y., AMIN U.N. (1996) – *Bearing mechanism of steel grid reinforcement in pull-out test.* International Symposium on Earth Reinforcement, Fukuoka, Kyushu, Japan, pp. 101-105.

MILLIGAN G.W.E., EARL R.F., BUSH D.I. (1990) – *Observations of photo-elastic pullout tests on geotextiles and geogrids.* 4th International Conference on Geotextiles, Geomembranes and Related Products, pp. 747-751.

MIRMORADI S.H., EHRLICH M., DIEGUEZ C. (2016) – *Evaluation of the combined effect of toe resistance and facing inclination on the behavior of GRS walls.* Geotextiles and Geomembranes, 44, pp. 287-294.

MIYATA Y., BATHURST R.J., ALLEN T.M. (2014) – *Reliability analysis of geogrid creep data in Japan.* Soils and Foundations, 54, pp. 608-620.

MORACI N. (2011) – *Il rinforzo del terreno con geosintetici - recenti sviluppi tecnologici, progettuali e normativi.* XXIV Convegno Nazionale Geotecnica - Innovazione Tecnologica nell'Ingegneria Geotecnica, Napoli, 52 p.

MORACI N., CARDILE G. (2008) – *Pullout behaviour of different geosynthetics embedded in granular soils.* 4th Asian Regional Conference on Geosynthetics, Shanghai, China, pp. 146-150.

MORACI N., CARDILE G. (2009a) – *Influence of cyclic tensile loading on pullout resistance of geogrids embed-*

ded in a compacted granular soil. Geotextiles and Geomembranes, 27, pp. 475-487.

MORACI N., CARDILE G. (2009b) – *The use of pullout test results in the serviceability limit states design of earth reinforcement structures.* GeoAfrica, Cape Town, 6 p.

MORACI N., CARDILE G. (2012) – *Deformative behaviour of different geogrids embedded in a granular soil under monotonic and cyclic pullout loads.* Geotextiles and Geomembranes, 32, pp. 104-110.

MORACI N., CARDILE G., GIOFFRÈ D. (2007) – *A theoretical method to predict the pullout behaviour of extruded geogrids embedded in granular soils.* 5th International Symposium on Earth Reinforcement, Fukuoka, Japan, 6 p.

MORACI N., CARDILE G., GIOFFRÈ D., MANDAGLIO M.C., CALVARANO L.S., CARBONE L. (2014a) – *Soil geosynthetic interaction: design parameters from experimental and theoretical analysis.* Transportation Infrastructure Geotechnology, 1, pp. 165-227.

MORACI N., CARDILE G., PISANO M. (2017) – *Soil-geosynthetic interface behaviour in the anchorage zone [Comportamento all'interfaccia terreno-geosintetico nella zona di ancoraggio].* Rivista Italiana di Geotecnica, 51, n. 1, pp. 5-25.

MORACI N., CAZZUFFI D., CALVARANO L.S., CARDILE G., GIOFFRÈ D., RECALCATI P. (2014b) – *The influence of soil type on interface behavior under pullout conditions.* Geosynthetics, 32, pp. 42-50.

MORACI N., GIOFFRÈ D. (2006) – *A simple method to evaluate the pullout resistance of extruded geogrids embedded in a compacted granular soil.* Geotextiles and Geomembranes, 24, pp. 198-199.

MORACI N., MONTANELLI F. (1995) – *Comportamento a breve e lungo termine di due geosintetici con funzione di rinforzo.* In: AGI (Ed.), XIX Convegno nazionale di Geotecnica - Il miglioramento e il rinforzo dei terreni e delle rocce, Pavia, Italy, pp. 369-380.

MORACI N., MONTANELLI F. (1997) – *Behavior of geogrids under cyclic loads.* Geosynthetics '97, Long Beach, CA, USA, 16 p.

MORACI N., MONTANELLI F. (2000) – *Analisi di prove di sfilamento di geogriglie estruse installate in terreno granulare compattato.* Rivista Italiana di Geotecnica, 4, pp. 5-21.

MORACI N., RECALCATI P. (2006) – *Factors affecting the pullout behaviour of extruded geogrids embedded in compacted granular soil.* Geotextiles and Geomembranes, 24, pp. 220-242.

NF P 94-270 (2009) – *Renforcement des sols. Ouvrages en sol renforcé par armatures ou nappes extensibles et souples.* Dimensionnement. Editions AFNOR, 182 p.

O'KELLY B.C., NAUGHTON P.J. (2008) – *On the interface shear resistance of a novel geogrid with in-plane drainage capability.* Geotextiles and Geomembranes, 26, pp. 357-362.

PALMEIRA E.M. (2004) – *Bearing force mobilisation in pullout tests on geogrids.* Geotextiles and Geomembranes, 22, pp. 481-509.

PALMEIRA, E.M. (2009) – *Soil–geosynthetic interaction: modelling and analysis.* Geotextiles and Geomembranes, 27, pp. 368-390.

PALMEIRA E.M., MILLIGAN G.W.E. (1989a) – *Scale and other factors affecting the results of pullout tests of grid buried in sand.* Géotechnique, 39, n. 3, pp. 511-524.

PALMEIRA E.M., MILLIGAN G.W.E. (1989b) – *Large scale direct shear tests on reinforced soil.* Soils and Foundations, 229, n. 1, pp. 18-30.

PALMEIRA E.M., TATSUOKA F., BATHURST R.B., STEVENSON P.E., ZORNBERG J.G. (2008) – *Advances in geosynthetics materials and applications for soil reinforcement and environmental protection works.* Electronic Journal of Geotechnical Engineering, 13, pp. 1-38.

PENG F.-L., LI F.-L., TAN Y., KONGKITKUL W. (2010) – *A rate-dependent constitutive model for polymer geosynthetics.* Mechanics Research Communications, 37, pp. 384-388.

PERKINS S.W. (1999) – *Mechanical Response of Geosynthetic-Reinforced Flexible Pavements.* Geosynthetics International, 6, pp. 347-382.

PERKINS S.W., CUELHO E.V. (1999) – *Soil-geosynthetic interface strength and stiffness relationships from pullout tests.* Geosynthetics International, 6, pp. 321-346.

PERKINS S.W., ISMEIK M. (1997a) – *A Synthesis and Evaluation of Geosynthetic-Reinforced Base Layers in Flexible Pavements- Part I.* Geosynthetics International, 4, pp. 549-604.

PERKINS S.W., ISMEIK M. (1997b) – *A Synthesis and Evaluation of Geosynthetic-Reinforced Base Layers in Flexible Pavements- Part II.* Geosynthetics International, 4, pp. 605-621.

PETERSON L.M., ANDERSON L.R. (1980) – *Pullout resistance of welded wire mats embedded in soil.* Hilfiker Company, 106 p.

PISANO M., CARDILE G., MORACI N. (2019) – *Soil-geogrid interface behaviour under cyclic pullout conditions.* In F. Silvestri, N. Moraci (Eds.), "Earthquake geotechnical engineering for protection and development of environment and constructions", 7th International Conference on Earthquake Geotechnical Engineering (Roma, 17-20 giugno 2019), CRC Press, Boca Raton, London, New York 2019, pp. 4507-4514.

PWRC (2013) – *Design and construction manual of geosynthetics reinforced soil.* Public Works Research Center, Tsukuba, Ibaraki, Japan, 305 p. (in Japanese).

RTRI (2007) – *Design standard for railway structures. Railway.* Railway Technical Research Institute, Technical Research Institute Maruzen, pp. 47 and 89-90.

SANDRI D. (1997) – *A performance summary of reinforced soil structures in the greater Los Angeles Area after the Northridge Earthquake.* Geotextiles and Geomembranes, 15, pp. 235-253.

SCHMID I., KAZDA M. (2001) – *Vertical distribution and radial growth of coarse roots in pure and mixed stands of Fagus sylvatica and Picea abies*. Canadian Journal of Forest Research, 31, pp. 539-548.

SHUKLA S.K., CHANDRA S. (1994) – *A generalized mechanical model for geosynthetic-reinforced foundation soil*. Geotextiles and Geomembranes, 13, pp. 813-825.

SHUKLA S.K. (2016) – *An introduction to Geosynthetic Engineering*. CRC Press, Taylor and Francis, 466 p.

SUGIMOTO M., ALAGIYAWANNA A.M.N., KADOGUCHI K. (2001) – *Influence of rigid and flexible face on geogrid pullout tests*. Geotextiles and Geomembranes, 19, pp. 257-277.

TATSUOKA F. (2008) – *Geosynthetics engineering, combining two engineering disciplines*. 4th Geosynthetics Asia - Special Lecture, Shanghai, Cina, pp. 1-35.

TATSUOKA F., HIRAKAWA D., SHINODA M., KONGKITKUL W., UCHIMURA T. (2004) – *An old but new issue; Viscous properties of polymer geosynthetic reinforcement and geosynthetic-reinforced soil structures*. 3rd Asian Regional Conference on Geosynthetics, Seoul, Korea, pp. 29-77.

TATSUOKA F., KOSEKI J., KUWANO J. (2014) – *Natural disasters mitigation by using construction methods with geosynthetics (Earthquakes)*. 10th International Conference on Geosynthetics, ICG 2014, pp. 80-132.

TATSUOKA F., KOSEKI J., TATEYAMA M. (1995) – *Performance of geogrid-reinforced soil retaining walls during the Great Hanshin-Awaji Earthquake, January 17, 1995*. 1st International Symposium on Earthquake Geotechnical Engineering, Earthquake Geotechnical Engineering Journal, pp. 55-62.

TATSUOKA F., KOSEKI J., TATEYAMA M. (1997) – *Performance of reinforced soil structures during the 1995 Hyogo-ken Nanbu Earthquake*. Balkema, Rotterdam, pp. 973-1008.

TATSUOKA F., TATEYAMA M., MOHRI Y., MATSUSHIMA K. (2007) – *Remedial treatment of soil structures using geosynthetic-reinforcing technology*. Geotextiles and Geomembranes, 25, pp. 204-220.

THUO J.N., YANG K.H., HUANG C.C. (2015) – *Infiltration into unsaturated reinforced slopes with nonwoven geotextile drains sandwiched in sand layers*. Geosynthetics International, 22, pp. 457-474.

TOUZE-FOLTZ N., BANNOUR H., BARRAL C., STOLTZ G. (2016) – *A review of the performance of geosynthetics for environmental protection*. Geotextiles and Geomembranes, 44, pp. 656-672.

UNI EN ISO 10319 (2015) – *Geosynthetics – Wide-width tensile test. - Geosintetici - Prova di trazione a banda larga*. Ente Nazionale Italiano di Unificazione, Milano.

UNI EN ISO 13286-2 (2010) – *Miscele non legate e legate con leganti idraulici – Parte 2: Metodi di prova per la determinazione della massa unica e del contenuto di acqua di riferimento di laboratorio – Costipamento Proctor*. Ente Nazionale Italiano di Unificazione, Milano.

UNI EN ISO 14688-1 (2018) – *Indagini e prove geotecniche - Identificazione e classificazione dei terreni - Parte 1: Identificazione e descrizione*. Ente Nazionale Italiano di Unificazione, Milano.

WALLBAUM H., BÜSSER S., ITTEN R., FRISCHKNECHT R. (2014) – *Environmental benefits by using construction methods with geosynthetics*. 10th International Conference on Geosynthetics, ICG 2014, pp. 50-63.

WALTERS D.L., ALLEN T.M., BATHURST R.J. (2002) – *Conversion of geosynthetic strain to load using reinforcement stiffness*. Geosynthetics International, 9, pp. 483-523.

WANG Z., JACOBS F., ZIEGLER M. (2014) – *Visualization of load transfer behaviour between geogrid and sand using PFC2D*. Geotextiles and Geomembranes, 42, pp. 83-90.

WARTMAN J., RONDINEL-OVIEDO E.A., RODRIGUEZ-MAREK A. (2006) – *Performance and analyses of mechanically stabilized earth walls in the Tecomán, Mexico Earthquake*. Journal of Performance of Constructed Facilities, 20, pp. 287-299.

WHITE D.M., HOLTZ R.D. (1994) – *Performance of geosynthetic-reinforced slopes and walls during the Northridge, California Earthquake of January 17, 1994*. International Symposium on Earth Reinforcement, IS-Kyushu '96, Fukuoka, Kyushu, Japan, pp. 965-972.

WORLD COMMISSION ON ENVIRONMENT AND DEVELOPMENT (1987) – *Our Common Future*. Oxford University Press, 300 p.

WU H., HUANG B., SHU X., ZHAO S. (2015) – *Evaluation of geogrid reinforcement effects on unbound granular pavement base courses using loaded wheel tester*. Geotextiles and Geomembranes, 43, n. 5, pp. 462-469.

YANG S.-H., AL-QUADI I.L. (2007) – *Cost-effectiveness of using geotextiles in flexible pavements*. Geosynthetics International, 14, pp. 2-12.

YONEZAWA T., YAMAZAKI T., TATEYAMA M., TATSUOKA F. (2014) – *Design and construction of geosynthetic-reinforced soil structures for Hokkaido high-speed train line*. Transportation Geotechnics, 1, pp. 3-20.

ZHOU J., CHEN J.-F., XUE J.-F., WANG J.-Q. (2012) – *Micro-mechanism of the interaction between sand and geogrid transverse ribs*. Geosynthetics International, 19, pp. 426-437.

ZIEGLER M., TIMMERS V. (2004) – *A new approach to design geogrid reinforcement*. 3rd European Geosynthetics Conference, Munich, Germany, R. Floss, G. Bräu, M. Nußbaumer (Eds.), Munich, DGGT, 2, pp. 661-666.

ZORNBERG J.G., KANG Y. (2005) – *Pullout of geosynthetic reinforcement with in-plane drainage capability*. Geosynthetics Research and Development in Progress - Geo-Frontiers 2005, 6 p.

ZORNBERG J.G., KAVAZANJIAN JR E. (2001) – *Prediction of the performance of a geogrid-reinforced slope founded on solid waste*. Soils and Foundations, 41, pp. 1-16.

Avanzamenti nel campo del rinforzo del terreno con geosintetici: dalle prove di laboratorio alla pratica progettuale

Sommario

Nell'ambito della definizione di strategie di sviluppo sostenibile il presente articolo fornisce una panoramica aggiornata sul ruolo dei geosintetici aventi funzione di rinforzo. Data la vastità dell'argomento il campo sarà ristretto ad alcune applicazioni, nello specifico ai muri e ai pendii ripidi rinforzati con geosintetici, in cui la struttura è costruita alternando strati di terreno compattato a geosintetici risvoltati o connessi alla facciata (in calcestruzzo gettato in opera o costruita montando insieme blocchi o pannelli in calcestruzzo prefabbricati).

La sperimentazione, sia essa intesa come sviluppo ed esecuzione di prove di laboratorio sull'elemento di volume rappresentativo o come analisi del comportamento di opere in vera grandezza opportunamente strumentate, ha rappresentato e rappresenta tutt'oggi per questa disciplina la base di partenza nonché il motore dei continui progressi registrati. Per tali ragioni, l'articolo sarà sviluppato partendo proprio dai risultati che la ricerca recente ha prodotto sulla definizione dei parametri di progetto a breve e lungo termine, studiati in laboratorio attraverso apparecchiature (spesso prototipo) di grandi dimensioni. I risultati sperimentali ottenuti saranno interpretati tenendo conto dei meccanismi di interazione elementare effettivamente mobilitati lungo l'interfaccia terreno-geosintetico. Successivamente, gli Autori analizzeranno come tali avanzamenti si siano tradotti o potranno tradursi in un avanzamento nella pratica progettuale.